

# Hadron interactions in cosmic rays at energies above the accelerator range

S. I. Nikol'skiĭ

*P. N. Lebedev Physics Institute, Academy of Sciences of the USSR  
Usp. Fiz. Nauk 135, 545-585 (December 1981)*

Experimental data on inelastic collisions of nucleons, pions, and nuclei in the energy range  $1-10^6$  TeV have been used for analysis of the dependence of the multiple production of hadrons on the energy of the incident hadron. The general pattern of inelastic hadron collisions is characterized by approximate scale invariance in the energy region  $1-100$  TeV and by a significant difference of the multiple-production process from that observed at accelerator energies in a number of the mean parameters, such as the multiplicities and composition of the secondary particles and their transverse momenta.

PACS numbers: 13.85.Mh, 13.85.Hd, 94.40.Rc

## CONTENTS

1. Introduction .....	925
2. Experimental apparatus for study of cosmic rays with energy of $10-10^4$ TeV .....	926
3. Energy spectrum and composition of primary cosmic radiation .....	927
4. Inelastic collisions of nucleons with nuclei in the energy region $1-10^2$ TeV .....	928
5. Can the observed characteristics of the multiple-production process be extrapolated to the energy region $10^2-10^5$ TeV? .....	932
6. Dependence of transverse momenta of secondary hadrons on the energy of the colliding particles .....	933
7. H-quanta, SH-quanta, centaurs, geminions, etc. ....	935
8. Some results of the Pamir experiment .....	939
9. Development of extensive air showers in the atmosphere .....	940
10. Nature of secondary particles in multiple-production events .....	942
11. Role of new particles in hadron cascades .....	944
12. Conclusion .....	946
References .....	947

## 1. INTRODUCTION

Cosmic rays enable us to look into the future of research in elementary-particle physics with accelerators. This possibility is the consequence of the single indisputable advantage of cosmic rays over accelerators—the presence in the cosmic-ray flux of particles with energy much greater than the particle energy attainable either in contemporary or in future accelerators. However, the many deficiencies of cosmic-ray experiments, due primarily to the low intensity, which falls off rapidly with increase of energy, have the consequence that the anticipatory nature of the investigations becomes preliminary. The results of cosmic-ray experiments for the most part bring out only the main characteristic features of inelastic collisions of hadrons but do not provide a detailed quantitative description of a multiple-production event.

It is hardly possible to give a complete review of the existing experimental data on hadron interactions above 2 TeV. It is also unreasonable to restrict the discussion to any given period of time. It is more appropriate to give a subset of experimental data which describes the general picture of inelastic hadron processes at ultrahigh energies. In view of the incompleteness of the experimental information such an approach can turn out to be subjective. It is permissible only because there are no sufficiently complete theoretical predictions regarding the characteristics of an inelastic collision and multiple production in the expected energy region.

Since the analysis and interpretation of many of the experimental results involves the characteristics of the energy spectrum and the composition of the primary radiation, at the beginning of the article we have given a summary of the principal data on primary cosmic rays. In the subsequent description of the experimental results on study of inelastic collisions of hadrons and, correspondingly, multiple-production processes, two groups of questions will be distinguished. First we shall discuss to what degree and up to what energies it is possible to speak of approximate scale invariance of the characteristics of hadron inelastic collisions. Second, what essentially distinguishes multiple-production processes in hadron collisions in the energy region above 100 TeV and processes in the energy region  $\leq 1$  TeV which have been studied in detail in accelerators.

The concentration of attention of processes in the energy region near 100 TeV is determined by two circumstances. First, the results of cosmic-ray investigations from the earliest studies permit us to speak of energies  $\sim 100$  TeV as certain limiting energies at which the general pattern of the multiple-production process changes. This may be one of the main results obtained in cosmic rays during the last twenty years. Second, the energy region  $10^2-10^3$  TeV will in the very near future become the region of investigation in the colliding beams at CERN and other centers of high-energy physics research. Therefore it is quite timely to outline the picture of inelastic collisions corresponding to ex-

periments in cosmic rays in just this energy range.

## 2. EXPERIMENTAL APPARATUS FOR STUDY OF COSMIC RAYS WITH ENERGY OF $10\text{--}10^4$ TeV

Experiments intended for study of hadron interactions in cosmic rays must take into account two features of the cosmic radiation: the low intensity and the broad energy spectrum of the hadrons.

The low intensity limits the choice of radiation detectors and is the reason for the popularity of x-ray emulsion chambers: a special type of x-ray film permits year-long exposures and relative economy for use in large areas (up to  $1000\text{ m}^2$ ).

The wide energy spectrum of the incident hadrons forces us to provide for measurement of the energy of the interacting particle. The best method of determining the energy of the primary particles which have produced an interaction in a target or in the atmosphere is the calorimetric method, employing ionization and scintillation calorimeters, and also the method of Cherenkov radiation of extensive air showers in the air above the level of measurement. Other methods of selecting interactions on the basis of the energy of the primary particles contain major *a priori* assumptions and are less accurate.

Examples of x-ray emulsion chambers<sup>1,2</sup> are given in Fig. 1. Inelastic collisions of hadrons in the atmosphere or in the target material lead to appearance of neutral pions. The photons from decay of the  $\pi^0$  mesons initiate electron-photon cascades which, developing in lead, leave a blackened spot on a special x-ray film pressed against the lead. For a cascade energy above 1 TeV near the maximum of the shower development, such spots can be seen by the unaided eye. Photometry permits determination of the cascade energy; the accuracy in measurement of the coordinates of the spot depends on the energy and amounts to  $\sim 10\text{ }\mu\text{m}$ . The upper layers of x-ray film, which are interleaved with layers of lead every 2–4 radiation lengths, record electron-photon showers which develop from photons and electrons which hit the apparatus from the atmosphere. The electrons and photons coming from the atmosphere can be separated from hadrons which interact in the material of the x-ray emulsion chamber on the basis of the depth of formation of the cascade, with use of the large difference between the radiation length ( $\sim 6.4\text{ g/cm}^2$ ) and the range for hadron collisions ( $\sim 200\text{ g/cm}^2$ ) in lead. For more efficient separation of had-

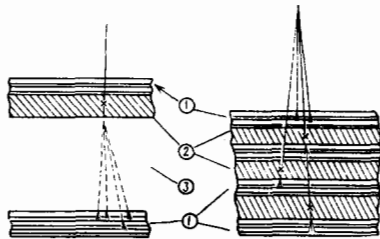


FIG. 1. X-ray emulsion chambers used in study of electron-photon and hadron cascades with initial energy  $10\text{--}10^4$  TeV. 1—layers of lead and x-ray film, 2—carbon target, 3—air space between upper and lower blocks.

rons, under the upper x-ray emulsion chamber is placed a layer of carbon-containing material in the form of a target in which electron-photon cascades develop only weakly. The thickness of the target is from one-third of the interaction range in the experiments at Chacaltaya<sup>1</sup> to a thickness equal to the range in the experiments in the Pamirs.<sup>2</sup> Under the target is placed an x-ray emulsion chamber for detection of the electron-photon cascades produced by hadrons in the material of the upper chamber, the target, and the lead below the chamber. Between the carbon target and the lower chamber in the Chacaltaya experiment there is a free space in which secondary particles originating in interactions in the upper part of the apparatus can spread out in space and become resolvable in the lower chamber. In the Pamir experiment there is no such space. In addition to the x-ray film, in part of the experiments to reduce the energy threshold for detection of electron-photon cascades, nuclear emulsions were used. The areas of these installations amount to tens of square meters at Chacaltaya and hundreds of square meters at the Pamirs.

The Tien Shan comprehensive installation<sup>3</sup> for study of extensive air showers and hadron interactions is shown in Fig. 2. Extensive air showers consist of a large number of electrons, photons, muons, and hadrons which have multiplied as the result of a cascade of interactions of hadrons, electrons, and photons with the nuclei of the atoms of the atmosphere when high-energy cosmic radiation hits the top of the atmosphere. The electrons, photons, and muons of low energy are scattered to large distances from the shower axis (the ex-

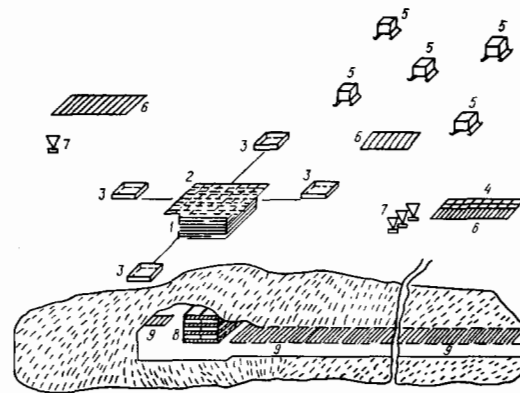


FIG. 2. Tien-shan comprehensive installation for extensive air showers.<sup>3</sup> The central part of the apparatus consists of: 1—ionization calorimeter, 2—"carpet" of scintillation counters, 3—scintillation counters for determination of relative time of arrival of particles, 8—spark chambers and ionization calorimeter for study of high-energy muons and of the cores of large showers. Scintillators 4 and 5 and spark counters 6 measure the flux of the electron-photon component of the shower at distances 30–200 m from the shower axis, 7—detectors for Cherenkov flash in the atmosphere, 9—counter hodoscope for measurement of muon flux at various distances from the shower axis. The complex is controlled by scintillation detectors 2 and 3 (the shower axis at the center) and scintillation detectors 5 (the shower axis at a distance 50–70 m from the detectors of muons with energy  $\geq 5$  GeV in the central part of the installation).

tension of the primary-particle trajectory). Use of shower-particle detectors separated by hundreds of meters permits recording of extremely rare extensive showers produced by primary particles with energy of  $10^6$ – $10^8$  TeV. However, for study of inelastic collisions of high-energy hadrons, more valuable information is contained in the central part of the shower, the core, where there is a concentration of the high-energy particles which best reflect the picture of the first interactions in the shower development. Thus, it is just the central part of the apparatus (see Fig. 2) with its ionization calorimeter which determines the luminosity of the apparatus. The area of the ionization calorimeter of the installation shown in Fig. 2 is  $36 \text{ m}^2$ . The calorimeter is used to measure the energy of the electron-photon and hadron components of the shower core, and the structure of the core and the central part of the shower is brought out with resolution of multiple cores, jets, and individual hadrons which are separated by more than  $0.3 \text{ m}$ . Scintillation counters above the calorimeter serve to determine the coordinates of the shower axis on the basis of the total flux of the electron-photon component. The accuracy in determination of the axis is of the order of the distance between the closest detectors. Scintillation counters located at a distance  $\sim 20 \text{ m}$  from the center of the apparatus, in addition to measuring the electron flux density at the corresponding distances, on the basis of the difference in time of arrival of the particles at these detectors permit determination of the location of the shower front and from this the zenith and azimuthal angles of the shower axis. The possibility in each shower with a primary energy above  $10^2 \text{ TeV}$  of knowing the flux of electrons at all distances from the core up to  $\sim 70 \text{ m}$  is extremely important for analysis of the data, since at these distances the greater part of the total number of particles at the level of measurements is concentrated. This number is an excellent classification parameter and physical parameter of the shower. Hodoscopic counters in a tunnel under an earth layer of thickness about  $20 \text{ m}$  of water equivalent (mwe) are intended for determination of the flux of muons with energy above  $5 \text{ GeV}$  in the shower. The ratio of the fluxes of muons and electrons in an extensive air shower is sensitive to the nature of the primary particle which produced the shower. Although detectors of Cherenkov radiation arising in the atmosphere in passage of the shower are effective only about  $10\%$  of the time of operation of the apparatus, since measurements are possible only on clear, moonless nights, their role is important, since the Cherenkov radiation above the level of observation reflects the energy loss by the shower electrons above the measurement level. This energy amounts to more than half of the energy of the particle which produced the shower, which permits evaluation of the energy of the primary particle with extremely weak assumptions regarding the model of the strong interaction. Spark chambers and an ionization calorimeter in the underground laboratory are used for study of high-energy muons in the cores of extensive air showers. It should be noted that the large ionization calorimeter in combination with the shower-particle detectors provides the possibility of studying interactions of protons of the primary radiation by distinguish-

ing hadron cascades in the calorimeter without accompaniment by a shower in the atmosphere on the basis of the absence of shower particles in the scintillators and hodoscopic counters above the calorimeter.

### 3. ENERGY SPECTRUM AND COMPOSITION OF PRIMARY COSMIC RADIATION

The interval of energies of the primary cosmic radiation which is important for the questions considered in the present article extends from one up to  $10^8 \text{ TeV}$  per nucleon or, with allowance for the nuclear composition of the primary particles, approximately up to  $10^6 \text{ TeV}$  per particle. In the initial part of this energy interval the only direct measurements of the intensity of the primary cosmic radiation are measurements in the Proton satellites,<sup>4</sup> and reliable data on the composition exist only at the lower energy limit.<sup>5</sup> However, this energy interval as a whole is investigated by indirect methods, mainly by study of extensive air showers arising on entry of primary protons and nuclei into the atmosphere.

In Fig. 3 we have shown the principal experimental data on the energy spectrum of the total flux of primary cosmic radiation in the range of energies  $1$ – $10^6 \text{ TeV}$ . The intensity of the flux of particles with energy above a given value  $F(>E)$  is multiplied by  $E^2$  for better representation of the data at different energies, which differ in the values of the particle flux by more than  $10^{10}$  times. As can be seen from the figure, the experimental data are fairly well fitted by the relations

$$F(>E) = 7.2 \cdot 10^{-2} E^{-1.66} [(1 + 10^{-3} E)^{-0.34} + \sum_A \frac{B_A}{A} (1 + 2 \cdot 10^{-3} A^{-1} E)^{-0.34}] (\text{m}^2 \text{ sec}^{-1} \text{ sr}^{-1}), \quad (3.1)$$

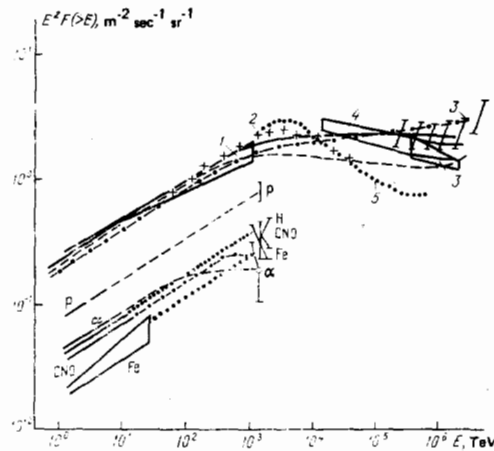


FIG. 3. Energy spectrum of primary cosmic radiation. The quantity  $E^2 F(>E)$  is plotted along the ordinate. The experimental data on the total flux of particles (1) were obtained in balloons<sup>4</sup> and satellites.<sup>4</sup> The data on extensive air showers are as follows: 2—Ref. 15, 3—Refs. 7 and 8, 4—Refs. 9 and 10, 5—Ref. 11. The dot-dash and dashed fits correspond to a change of the energy spectrum of all particles at a given magnetic rigidity (the formula in the text and in the review of Ref. 12); as in the curves of the partial spectra, the solid line corresponds to the assumptions of Ref. 13. The data on the fluxes of Fe nuclei and of the group H, CNO, and  $\alpha$  particles and on the primary photons have been taken from Refs. 5, 14, and 16.

$$F(>E) = 8.6 \cdot 10^{-2} E^{-1.03} [(1 \pm 5 \cdot 10^{-4} E)^{-0.35} + \sum_{A>1} B_A (1 + 3 \cdot 10^{-2} EA^{-1})^{-0.35}] \text{ (m}^{-2} \text{ sec}^{-1} \text{ sr}^{-1} \text{)}; \quad (3.2)$$

here  $E$  is the energy of the primary particle in TeV and  $B_A$  is the flux of nuclei with atomic weight  $A > 1$  at  $E = 1$  TeV relative to the flux of protons of the same energy. The summation is carried out over all  $A > 1$ .

The contemporary experimental data do not permit choice of the fit to the primary-particle energy spectrum closest to reality among those given in Fig. 3. From the point of view of their practical use, they are close together. This is determined by the principal experimental results which have been taken into account in selection of the parameters of the formulas. All the approximations connect the results of measurements of the absolute intensity of the primary-particle flux in three energy regions: in the energy interval 1–10 TeV at the edge of the atmosphere,<sup>4,6</sup> and in the regions of energies  $10^3$  and  $10^6$  TeV on the basis of the Cherenkov radiation of extensive air showers.<sup>7,15</sup> In addition, the change in the energy spectrum of the primary particles in the transition from energies below  $10^3$  TeV to energies above  $10^4$  TeV observed in the spectra of extensive air showers on the basis of the number of particles at sea level has been taken into account.<sup>11</sup>

The difference in the formulas is due to the assumptions regarding the reasons for the change in the energy spectrum in the energy region  $10^3$ – $10^4$  TeV. The formula (3.1) and those from our 1975 review<sup>12</sup> correspond to the assumption of a relation between the observed change in the spectrum and a dependence of the diffusion coefficient for cosmic rays in the magnetic fields of the Galaxy on the energy of the particles. In this case changes in the primary-particle spectra for different  $A$  values should be expected at the same magnetic rigidity.

Equation (3.2) describes the energy spectrum in the case in which the cause of change in the spectrum is the energy loss by protons and nuclei in collisions with photons.<sup>13</sup> The energy threshold for photoproduction of pions from protons is 10–20 times higher than that for photodisintegration of nuclei. This has the result that the changes in the energy spectrum of the  $\alpha$  particles and a large part of the nuclei of the primary cosmic rays occur at lower energies than in the spectrum of primary protons.

The various assumptions regarding the cause of the change in the energy spectrum imply also differences in the composition of the primary cosmic radiation. In Table I we have given the percentage content of protons and groups of nuclei with various  $A$  values in the primary cosmic radiation, corresponding to Eq. (3.1) and (3.2) at energies of  $10^3$  and  $10^6$  TeV if the direct experimental data<sup>5</sup> on the composition of the primary cosmic radiation at energy  $\geq 1$  TeV are used. The table also gives the results of an investigation of the composition of primary cosmic rays by analysis of the fluctuations of the number of muons in extensive air showers with a given number of electrons.<sup>14,16</sup>

TABLE I. Composition of primary cosmic radiation for a given energy of the particles, in %.

A	1	4	14	26	51	
E, TeV						
1	40	19	14	15	12	Measurements of Ref. 5 Formula (3.1) Formula (3.2) Analysis of fluctuations <sup>14,16</sup>
$10^3$	36	19	15	16	14	
$10^3$	46	12	12	16	14	
$10^3$	$41 \pm 4$	$9 \pm 7$	$15 \pm 6$	$17 \pm 6$	$19 \pm 5$	
$10^6$	25	15	16	22	22	
$10^6$	51	9	11	14	15	Formula (3.1) Formula (3.2)

Concluding this section, we should note that all the still existing uncertainties in the energy spectrum and composition of the primary cosmic radiation do not prevent a quantitative analysis of the interactions of hadrons in the atmosphere and of cascade processes arising in passage of cosmic rays with energy of  $10$ – $10^5$  TeV through the atmosphere.

#### 4. INELASTIC COLLISIONS OF NUCLEONS WITH NUCLEI IN THE ENERGY REGION 1– $10^2$ TeV

The energy interval 1– $10^2$  TeV is interesting as being immediately adjacent to the accelerator region of interacting-nucleon energy which is being investigated at the present time. It is accessible for investigation in cosmic rays by various methods. Obviously first of all we must check here to what extent it is possible to extrapolate the relations which have been established for inelastic collisions of hadrons in accelerator experiments. The possibility of such extrapolation from lower energies to higher energies in cosmic rays has been known for a long time. This appears in the constancy of the average inelasticity coefficient of nucleons (the fraction of energy carried away by the nucleon with the highest energy after a nucleon-nucleon or nucleon-nucleus interaction), and in the long known approximate similarity of the energy spectra of the different components of cosmic rays in the interior of the atmosphere to the energy spectrum of the primary radiation. It is natural to consider these properties as the manifestation of scale invariance (scaling)—a property of the interaction which was subsequently established in accelerator experiments. Regarding strict scale invariance of multiple-production processes in inelastic collisions of hadrons, there is apparently nothing which can be said at any energy. Already in the accelerator region a rise is observed in the effective cross section for inelastic collisions of nucleons with increase of their energy, and also increased multiplicity, in comparison with that expected on the basis of scaling, in the pionization part of the energy spectrum of secondary particles for an incident-nucleon energy  $\geq 1$  TeV. As will be seen from the description which follows of the experimental results obtained in cosmic rays, the same pattern of processes associated with inelastic collisions of hadrons is preserved up to 50–100 TeV. In a qualitative sense we can speak of "quasiscaling", understanding this to mean that over the entire energy interval considered there is a preservation of the peripheral nature of hadron interactions, preferential production of pions among the secondary hadrons, practical constancy of the transverse momenta, and so forth.

The cross section for collision of protons with the nuclei of atoms of the atmosphere increases with energy, and this increase, when converted to the effective cross section for proton-proton collisions (if we take as a basis the Glauber method,<sup>17</sup> supplementing it with inclusion of inelastic screening<sup>18</sup>), leads to

$$\sigma_{pp} = 38.4 + 0.5 \ln^2 \frac{E}{137} (\text{mb}).$$

The experimental data which we have used here for inelastic collisions of protons with the nuclei of the atmosphere were obtained by measurement of the intensity of the flux of primary protons of various energies which have reached a given depth of the atmosphere without interactions with nuclei of air atoms (Fig. 4) The energy of the protons was determined by means of an ionization calorimeter. Events which were not accompanied by an extensive air shower were taken to be cases of primary protons travelling down to an atmospheric depth of  $\sim 700 \text{ g/cm}^2$ . The experimental dependence obtained by this means for the effective cross section for interactions of protons with air nuclei:

$$\sigma_{\text{exp}}^{\text{p-air}} = 265 \left[ 1 + 0.016 \left( \ln \frac{E}{80 \text{ GeV}} \right)^{1.5} \right] (\text{mb})$$

gives in the accelerator energy region values about 13 mb less than those measured directly. This is explained by the fact that in cosmic-ray measurements diffraction excitations of the nucleons of the target nucleus with a small energy loss by the incident proton are not recorded.<sup>19</sup> The experimental data in the proton-energy interval  $E = 1-30 \text{ TeV}$  are compared in Fig. 4 with the formula given above and also with other approximations which are used for analysis of experimental data over a wide range of energies. The limitations on the value of the cross section at energies  $\sim 10^5 \text{ TeV}$  were obtained by study of fluctuations in the development of extensive air showers.

The constancy of the loss of energy by the incident proton in formation of secondary particles in inelastic collisions with lead nuclei can be deduced from the energy dependence of the threshold inelasticity coefficient  $K_\gamma$ , which is the fraction of the incident-proton energy transferred after the collision into an electron-photon cascade. This occurs mainly by means of the genera-

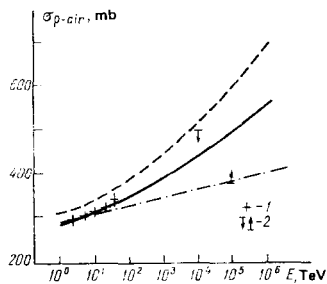


FIG. 4. Effective cross section for production of secondary particles in collisions with nuclei of air atoms as a function of the energy of the incident protons. Experimental data: 1— from Ref. 18, 2—from Refs. 20 and 21. The solid line is a fit with the formula in the text, the dot-dash line shows the fit from Ref. 22, and the dashed line the fit in the calculations of Ref. 23.

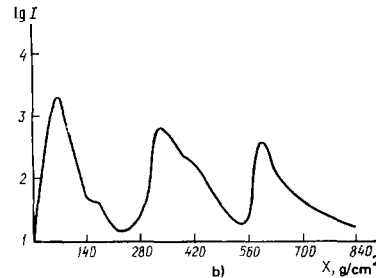
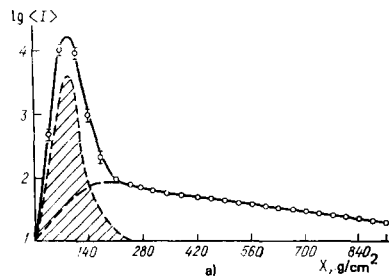


FIG. 5. Schematic representation of the ionization at various depths in the lead of the ionization calorimeter. a) Averaged curve for interactions at depth  $X=0$ . Crosshatched part—ionization from electron-photon cascades after the first interaction. b) Example of an individual nuclear cascade shower.

tion and decay of neutral pions. The use of lead as an absorber in an ionization calorimeter has turned out to be extremely effective for analysis of the characteristics of multiple-production events on the basis of the shape of the nuclear cascade curve in lead. The 30-fold difference in the nuclear interaction length and the radiation length permits separation in cascade curves, averaged over many events, of the initial part of these curves associated with the electron-photon cascade after the primary interaction of the nucleon in lead. The possibility also appears of distinguishing in individual cascades the ionization from the first interaction and that from subsequent interactions of the particle which is leading in energy of the secondary hadrons (Fig. 5).

In Fig. 6 we have shown the dependence on the incident-particle energy of the partial inelasticity coefficients  $\langle K_\gamma \rangle$  for primary protons (hadrons without accompaniment of an extensive air shower) and for a mixture in unknown proportion of nucleons and pions (all hadron interactions spatially resolved in the calorimeter).<sup>24</sup> From these measurements it follows that the quantity

$$\langle K_\gamma \rangle = \sigma^{-1} \int_0^1 x_{\pi^0} \frac{d\sigma_{\pi^0}}{dx_{\pi^0}} dx_{\pi^0}$$

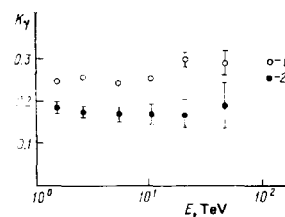


FIG. 6. Partial inelasticity coefficient as a function of energy for interactions of protons with lead nuclei (2) and of a mixture of protons and pions with lead nuclei (1).

averaged over many events is independent of the energy of the incident hadron up to energies  $\sim 30$  TeV. Here  $\sigma$  is the effective cross sections for production of secondary particles at an incident-particle energy  $E_0$  and  $x_{\pi^0} = E/E_0$  is the relative energy of the  $\pi^0$  mesons generated with an effective cross section  $d\sigma_{\pi^0}/dx_{\pi^0}$ . The quantity  $\langle K_\gamma \rangle$  in pion-nucleus collisions is larger than in nucleon-nucleus collisions. The value of  $\langle K_\gamma \rangle$  for a mixture of nucleons and pions is consistent with the fact that the partial inelasticity coefficient  $\langle K_\gamma \rangle$  in pion collisions with lead nuclei amounts to 0.3, and correspondingly the total inelasticity coefficient in such collisions is close to unity.

The result of measurement of the partial inelasticity coefficient in proton-nucleus collisions is significantly more definite. Its value averaged over the entire energy interval is  $\langle K_\gamma \rangle = 0.18 \pm 0.01$ . The constancy of this value, together with the constancy of the total inelasticity coefficient, reflects the identity of the composition of the greater part of the secondary hadrons over the entire energy region studied.

The total inelasticity coefficient can also be determined independently in a different way by analysis of the set of individual nuclear cascade showers in the lead of the ionization calorimeter. As the starting point of this analysis it is assumed that the main secondary peak in an individual distribution of ionization in the calorimeter is due to the interaction of the secondary nucleon which is leading in energy. The experimentally observed distribution of the relative values of the energy of interactions of particles responsible for the main secondary maximum is shown in Fig. 7. The initial assumption that the main secondary maximum is necessarily due to interaction of the leading nucleon is only a first approximation. For example, one of the most energetic secondary pions can give a maximum in the cascade curve which is no smaller than that from interaction of the leading nucleon. There is a probability also that the interaction of the leading nucleon will occur close to the point of the primary interaction of the nucleon in the ionization calorimeter. These and other less important corrections are introduced by

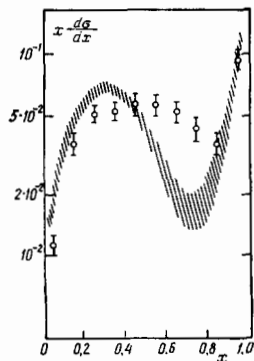


FIG. 7. Probability of appearance of a leading nucleon with a relative energy  $x = E/E_0 = 1 - k$  for collisions of protons with lead nuclei at an energy  $\langle E_0 \rangle = 7$  TeV. The circles are the measured ratio of the energy of the principal secondary interaction to the total energy, and the crosshatched band is the result after corrections.

successive approximations in modeling of the nuclear cascade curves by computer. Here the analysis is carried out according to the same program as for the data obtained experimentally. The corrected inclusive spectrum of leading nucleons ( $P + A = N + \dots$ ) at an initial proton energy of 5–10 TeV is shown in Fig. 7 by the cross-hatched band.<sup>25</sup> The average value of the total inelasticity coefficient obtained from the distribution presented is  $0.63 \pm 0.02$ . The difference of this value from  $3\langle K_\gamma \rangle = 0.54 \pm 0.03$ , if one sets aside the indicated error, is explained by the production in an inelastic collision of hadrons of a given energy, in addition to pions, of other particles, which is observed also at accelerator energies.

Unfortunately, experiments with lead as a target do not provide an answer as to what processes are responsible for and what energy loss by the interacting hadron is involved in the rise of the effective cross section with increasing energy of the incident particle in collisions with light nuclei. In complete correspondence with measurements of the energy dependence of the effective cross section in light nuclei and with the Glauber theory, the increase of the effective cross section for collisions of protons with lead nuclei in the energy interval 0.1–10 TeV does not exceed 10%. The experimental results agree with such estimates, but it is not possible to analyze how the inclusive spectra of secondary particles change with this insignificant increase of the cross section. It should be noted only that at an energy of 7–10 TeV diffraction processes in collisions of protons with lead nuclei have an effective cross section which is no smaller than at low energies (this is evident from the rise of the curve in Fig. 7 as  $x \rightarrow 1$ ).

The dependence of the inclusive spectrum of secondary particles in the fragmentation region on the energy of the nucleon which collides with light nuclei can be deduced from the energy spectra of hadrons,  $\gamma$  rays, and muons in the interior of the atmosphere. They are determined first of all by the energy spectra and composition of the primary cosmic radiations, second—by the energy dependences of the effective cross section for inelastic collision of nucleons and pions with air nuclei, and third—by the inclusive spectra of secondary hadrons, where a substantial role is played by the fragmentation part of these spectra. The latter is due to the fact that for the intensity of particles of a given energy in the interior of the atmosphere the following quantity is important:

$$\langle (x_\pi)^\gamma \rangle = \sigma^{-1} \int_0^1 (x_\pi)^\gamma \frac{d\sigma_\pi}{dx_\pi} dx_\pi.$$

The exponent of the primary energy spectrum  $\gamma = 1.7$  enhances the role of high energies, i.e., of the fragmentation part of the secondary-particle spectrum. A similar analysis has been carried out by many authors,<sup>22, 26-30</sup> who reached somewhat differing conclusions regarding the presence or absence of scaling in the fragmentation part of the secondary-particle spectrum for incident-hadron energies 1–100 TeV. The causes of the discrepancies are due to inaccuracies and sometimes also contradictions of the experimental data and to the fact that comparison of experiment and theory is

carried out only on the basis of one of the components of cosmic radiation. For example, the observed energy spectrum of muons can be obtained with approximately equal success theoretically with use of both a rising and a constant effective cross section for inelastic collisions,<sup>22</sup> on the assumption of scaling, and with an inclusive secondary-particle spectrum which depends on the primary energy.<sup>27</sup> In Fig. 8 we have given a comparison of calculations<sup>29</sup> on the basis of different models of an inelastic collision (for interaction parameters which are considered reasonable at the present time). It follows from the comparison that in this case the experimental errors and especially the differences between various experimental arrangements do not permit the values of the parameters of the elementary event to be improved. On the other hand, this weak sensitivity of the muon energy spectrum to the parameter values being discussed permits us to use the intensity of muons of various energies to establish the energy spectrum of the primary nucleons.

Let us consider a more complete set of data on the intensity of cosmic rays in the interior of the atmosphere. The energy spectrum and composition of the primary cosmic radiation in the energy interval 1–10<sup>3</sup> TeV have been determined by direct measurements, by analysis of data on extensive air showers, and from the energy spectrum of muons. The effective cross section for inelastic collisions is established from the penetration of the primary protons into the depth of the atmosphere without interactions. Consequently the energy spectra of hadrons, photons, and electrons in the interior of the atmosphere can be used for analysis of the dependence of the inclusive spectra of secondary hadrons on the energy of the incident particle in multiple-production events in collisions of nucleons and pions with air nuclei.

In Fig. 9 we have given a comparison of the experimental data on the flux of high-energy electrons and photons at mountain altitudes with a calculation with various assumptions regarding the inclusive spectra of

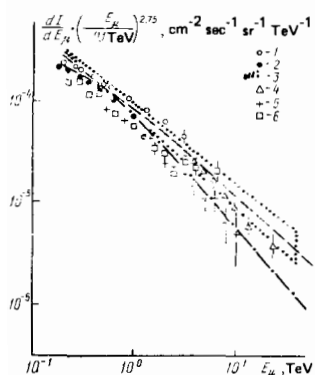


FIG. 8. Differential energy spectrum of the vertical flux of muons according to experimental data and calculations from Ref. 29. Dashed curve—on the assumption of scaling, dot-dash—with a secondary-pion spectrum of the Bose-Planck type. Experimental data: 1—from Ref. 31, 2—Ref. 32, 3—Ref. 33, 4—Ref. 34, 5—Ref. 35, 6—Ref. 36. The ordinate gives the spectrum multiplied by  $(E_\mu/0.1 \text{ TeV})^{2.75}$ .

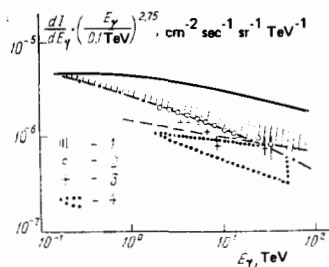


FIG. 9. Differential spectrum of electrons and photons in the atmosphere. Calculation<sup>29</sup> for a depth of 600 g/cm<sup>2</sup> on the assumption of scaling (solid curve), for a secondary-hadron spectrum of Bose-Planck type (dot-dash). Calculations<sup>37</sup> on the assumption of scaling violation in the pionization part and a rapid rise of the effective cross section (dashed curve). Experimental data: 1—depth in atmosphere 550 g/cm<sup>2</sup> from the data of Ref. 38, 2—depth 596 g/cm<sup>2</sup> from Ref. 39, 3—depth 700 g/cm<sup>2</sup> from the data of Ref. 40, 4—depth 650 g/cm<sup>2</sup> from the data of Ref. 41.

secondary hadrons.<sup>29</sup> In the case of preservation of scaling for the fragmentation part, the entire increase of the effective cross section was assigned to generation of secondary particles in the pionization region, and in the fragmentation part it was assumed that  $x d\sigma/dx = \text{const}$ . The variant without strict scaling, both in the pionization part and in the fragmentation part of the spectrum, is described by inclusive spectra of the Bose-Planck type. In the accelerator energy region these spectra, within experimental error, can be considered to be quasiscaling.<sup>42</sup> In analyses of data on extensive air showers this model has been used for a long time and is known as the Cocconi-Koester-Perkins (CKP) model with a dependence of the secondary-particle multiplicity on energy of the form  $n \sim E^0$ .<sup>25</sup> As can be seen in Fig. 9, the calculations with a nonscaling behavior of the inclusive spectra of secondary particles, both in the fragmentation part and in the pionization part, are close to the experimental data.

It should be noted that there have been many attempts to reconcile the experimental data with calculations on the assumption of preservation of scaling, and first of all that the fragmentation part of the secondary-particle energy spectrum is independent of the incident-hadron energy. The calculations of Ivanenko *et al.*<sup>22</sup> assumed for this a rapid increase of the effective cross section for inelastic interactions of nucleons with the nuclei of air atoms, more rapid than follows from measurements of the intensity of primary protons in the depth of the atmosphere.<sup>18</sup> The effective cross section for pion-nucleus interactions in these calculations is also overestimated. Dunaevskii *et al.*<sup>28</sup> propose to bring the calculations closer to the experimental data by assuming a decrease with increasing energy of the role of diffraction processes with small energy loss by the incident nucleon. This assumption does not correspond to the data<sup>25</sup> on interaction of protons with lead nuclei (see Fig. 7). Finally, taking into account that the flux of  $\gamma$  rays, electrons, and hadrons with a given energy in the depth of the atmosphere is produced by primary particles with energy 20–100 times greater, one can suggest an influence on the intensity of  $\gamma$  rays and hadrons with

energy  $\sim 10$  TeV of features of the interactions of hadrons at energies  $\sim 10^3$  TeV.<sup>30</sup> This variant deserves attention also because it will be shown below that there are new processes in the energy region above  $10^2$  TeV. Thus, summarizing the results of the study of multiple generation in hadron interactions at energies 1–100 TeV, we can state that the violations of scale invariance observed in this region reduce to the facts known from accelerator experiments of the rise in the effective collision cross section and the particle multiplicity in the pionization part of the inclusive spectrum. The inelasticity coefficient of nucleons and correspondingly the fragmentation part of their inclusive spectrum do not change with increase of the incident-nucleon energy. Changes of the fragmentation part of the inclusive spectra of secondary pions, if they exist, are insignificant. The composition of the secondary hadrons is for the most part constant both in number and in the energy flux: pions, kaons, and nucleons. The fraction of kaons, determined<sup>26</sup> from the angular distribution of muons to be  $\sim 15\%$ , agrees both with the accelerator data and with the difference noted above in the values  $3\langle K_\gamma \rangle$  and  $\langle K \rangle$ .

### 5. CAN THE OBSERVED CHARACTERISTICS OF THE MULTIPLE-PRODUCTION PROCESS BE EXTRAPOLATED TO THE ENERGY REGION $10^2$ – $10^5$ TeV?

The rise of the effective cross section corresponding to the limiting case for proton-proton collisions  $\sigma^{pp} = a + b \ln^2 s$ , and the inclusive spectra of secondary particles, which change with increase of the energy of the interacting particles in accordance with the CKP model which has long been used for analysis of extensive air showers, —all this information forces us to adopt a conservative approach in extrapolation of the characteristics of the hadron multiple-production process from the region of energy below 100 TeV to the energy region  $10^2$ – $10^5$  TeV. However, in cosmic rays, which have their own unique uncertainty in interpretation, the contradictions between experiment and the expected result are more informative than the absence of such contradictions would be. Therefore it seems preferable to take into account first of all those new aspects of multiple-production processes which come to light at energies  $\sim 100$  TeV and above.

The features of the pattern of inelastic collisions of nucleons and nuclei at energies above 100 TeV were noted quite long ago in analysis of the results of investigations of the composition of extensive air showers. Qualitatively, the disproportions in the various components of the shower reduced to disproportions in the energy transferred to the various components of the shower in comparison with the expected distribution for a nucleon-pion composition of the nuclear cascade. The preferential formation of the electron-photon component has been arbitrarily called gammanization.<sup>43</sup>

The difference from the expected behavior in the formation of the electron-photon component and the muons in a shower can be seen in the fact that the dependence of the secondary-particle multiplicity on the energy of the primary particle which produced the shower turns

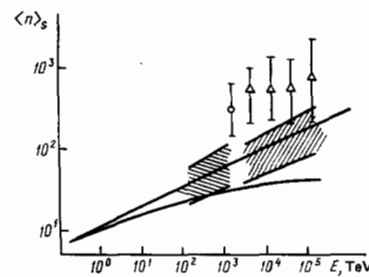


FIG. 10. Multiplicity of secondary pions as a function of the energy of the colliding hadron according to data on the height of the maximum of the development of the electron component of extensive air showers (points with error bars) and on the basis of the number of muons in a shower with a given number of electrons at the level of observation (cross-hatched bands). The lower curve was fitted on the assumption of scaling, and the straight line—on the assumption  $n \sim E^{1/4}$ .

out to be different for different means of its experimental determination. If this dependence is determined on the basis of the number of muons in showers with different numbers of electrons at a given level of observation, then it has to be close to  $n \sim E^{1/4}$ . However, if the secondary-pion multiplicity is estimated from the height of the maximum of the electron-photon component of the shower, then the experimental data correspond best to a dependence of the type  $n \sim E^{1/2}$  (Fig. 10). In order to remove this contradiction it is necessary to assume that the number of neutral pions in a multiple-production event is not equal to half of the number of charged pions or that there are other channels of transfer of energy from the primary nucleons to the electron-photon cascade of the shower.

The qualitative nature of the change in the pattern of the multiple-production process with increase of the energy of the colliding hadrons can be seen in the change of the average transverse momentum of the secondary particles. The energy region below 100 TeV is characterized by a weak dependence of the value of transverse momentum on energy. This result, which has been established in many experiments, may be due to the peripheral nature of inelastic collisions and to the large role of pions in the final stages of the emission of clusters. In the energy region above 100 TeV various authors<sup>44,45</sup> show, by analysis of the lateral distribution of hadrons in extensive air showers, not only that there are large values of the average transverse momenta of the secondary hadrons, but also that these values have a further substantial increase with increase of the colliding-particle energy (Fig. 11). The

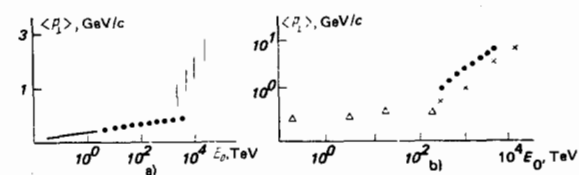


FIG. 11. Average transverse momenta of secondary hadrons as a function of the energy of the colliding nucleon: a) from Ref. 44, b) from Ref. 45.

transverse momenta will be described in more detail in the next section.

The energy threshold of the qualitative change in the secondary-particle production process appeared clearly in experiments on the absorption of hadronic cascades in lead for various initial energies.<sup>46</sup> Since the average absorption of the energy of the nucleon component in a hadronic cascade is characterized by an absorption range  $\leq \lambda/K = 2\lambda$ , and in an inelastic collision of pions two-thirds of the energy remains in the pionic shower, the absorption of the hadronic cascade on the whole is determined by the absorption of the pionic shower with a range  $L \leq \lambda'/0.33 = 3\lambda'$ ; here  $\lambda'$  is the range for interaction of a pion in lead. This simplified discussion emphasizes the fact that the absorption range of a hadronic shower for any initial energy is limited by irreversible energy losses in production of the electron-photon component of the shower if the nucleon-pion nature of the nuclear cascade is preserved. Actually there are a number of complicating factors. The rapid degradation of the energy of the pions in a shower has the result that the absorption cannot be described by an exponential. A significant part of the energy of a hadronic shower is expended in nuclear disintegrations. Kaons also take part in the nuclear cascade.

Since the role of these factors depends on the initial energy of the shower, the absorption of a shower will depend on the initial energy and will change with the depth of the absorber in which the shower develops. The main feature of showers which permits a rather reliable analysis of their absorption for different initial energies is related to the fact that all hadrons of the shower have energies less (and most of them much less) than the energy of the nucleon or pion which produced the shower. Thus, the properties of the particles which compose the shower are known. The preservation or change of these properties with increase of the energy of the nucleons and pions is traced by successive analyses of showers with ever increasing initial energies.

In Fig. 12 we have shown a comparison of experimental data on the absorption of showers for various initial energies with a calculation in which the specific experimental conditions<sup>47</sup> have been taken into account. The decrease of the absorption of hadronic showers for initial hadron energies  $\geq 100$  TeV signifies a substantial change in respect to energy of the composition of the

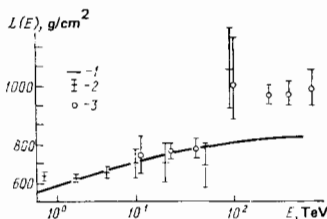


FIG. 12. Absorption range of a hadron shower in the lead of the ionization calorimeter as a function of the initial energy of the hadron shower. Curve 1—expected dependence, 2—experimental data on single hadrons, 3—cores of large showers.

secondary particles produced in inelastic collisions of hadrons with lead nuclei for increase of the energy up to 100 TeV. A minimum estimate of the energy carried away by "new" particles can be made on the basis of the observed excess of ionization in the depth of the calorimeter in comparison with that calculated for the usual nucleon-pion composition of the shower. The value obtained in this way amounts to  $>15\%$  of the energy of the hadron which produced the shower. It is difficult to suppose that the concentration of energy in one secondary particle exceeds 50% of the primary hadron energy. Accordingly the effective cross section for production of new particles is estimated to be  $>0.3\sigma$ , where  $\sigma$  is the effective cross section for an inelastic collision of the hadrons with nuclei. To explain the observed slow absorption of the showers it is necessary to assume that the new particles have a several times smaller effective cross section for inelastic collisions with lead nuclei and (or) a lower inelasticity coefficient. Of the known particles such properties can be assumed for charmed particles.<sup>48</sup>

The production of new particles with a large effective cross section essentially distinguishes inelastic collisions in the energy region  $\geq 100$  TeV from hadron interactions at lower energies.

## 6. DEPENDENCE OF THE TRANSVERSE MOMENTA OF THE SECONDARY HADRONS ON THE ENERGY OF THE COLLIDING PARTICLES

As we have already mentioned, a wide range of energy of inelastic collisions of hadrons is characterized by a very weak dependence of the secondary-particle transverse momenta on the incident-particle energy. Experimental indications of the presence of a significant number of events with large transverse momenta in interactions at energies  $\sim 10^3$  TeV were obtained in studies of the structure of the central part of extensive air showers.<sup>49,50</sup> Experiments showed that a fraction of extensive air showers have not one core corresponding to a maximum concentration of the particle flux around the shower axis, but two or more cores separated by distances of the order of 1 m. It is easy to estimate that, if the distance between the cores is assumed to result from the separation angles of the neutral pions or nucleons in the initial event at an elevation  $\sim 20$  km above the level of observation, it is necessary to assume an appreciable probability of appearance of transverse momenta  $\sim 10$  GeV/c. Of course, subsequent interactions are superimposed on the deviations of the leading, most energetic hadrons of an extensive air shower from the axis. Here the hadron energy becomes insignificantly smaller, but the distance to the level of observation at which for a given particle-emission angle the deviation from the shower axis is observed also becomes smaller. An extremely thorough analysis of the experimental data and a comparison with theory led a group of Australian physicists to the conclusion that the only possible explanation of the observed pattern of multicore showers is the assumption that high transverse momenta appear in interactions of nucleons at energies  $\sim 10^3$  TeV and that the transverse momenta increase with increase of the primary particle energy.<sup>51</sup>

However, although about ten years have passed since these authors drew this conclusion, which is reflected in Fig. 11, the problem of the dependence of the transverse momenta on the energy of the interacting particles remains in dispute. The objective difficulties in use of experimental data on multicore showers reduces to two experimental uncertainties: what energy must be assigned to each core, and what are the criteria for identification of multicore showers? The criteria for a multicore shower depend to a large degree on the experimental method and, depending on the characteristics of the apparatus itself, the fraction of multicore showers in various experiments differs by a several-fold factor. As a consequence of the change in the fraction of multicore showers, the estimates of the effective cross section for production of particles with large transverse momenta also change.

The first of the difficulties noted is determined by the relation between the number of electrons in the shower core at a radius of several tens of centimeters and the energy of the primary  $\gamma$  ray which produced the core. It depends greatly on the path in the atmosphere. Determination of the age of the shower within the distances indicated is also unreliable. The energy concentrated in the core of an electron-photon shower amounts to a small part of the energy of the total flux of particles at the level of observation and a still smaller part of the energy of the primary particle. All this is complicated by the presence in the shower of high-energy hadrons which can generate electron-photon cascades near the level of observation. The flux of energy and particles in such cascades can be concentrated in a circle of small radius, and if such cascades are erroneously taken as the core of an electron-photon cascade which has arrived from a great height, the error in the initial energy can amount to more than a factor of ten. A non-uniform distribution of matter above the apparatus, associated with the construction of the building where the apparatus is housed, also helps to produce such errors.

The difficulties described above are less characteristic for studies of the deviation of high-energy hadrons from the shower axis. The larger emission angles of hadrons, compared to the electromagnetic angles, in the production events and the multiple nature of the production result in the fact that hadrons of a given energy are efficiently recorded in interactions from small heights above the level of observation, and the greatest contribution to the deviation of the hadron from the shower axis is from its emission angle when it is produced. The sum of the deviations of the preceding interactions in a transverse-momentum distribution which does not depend on energy does not exceed 50% of the total deviation from the shower axis. Experimental studies<sup>45</sup> of the lateral distribution of hadrons in extensive air showers has shown that the data on hadrons with energy  $\leq 0.2$  TeV are consistent with a secondary-hadron transverse-momentum distribution which is independent of the primary-particle energy. This means, with allowance for the remark regarding the role of the last collision and the energy of the observed hadrons, that there is an independence or a weak dependence of the average transverse momentum

in the range of energies of the hadron interacting with the nucleus of an air atom 0.2–10 TeV. The experimental data on the lateral distribution of hadrons with energy above 1 TeV require for their explanation the assumption of a rise of the average transverse momentum, as is shown in Fig. 11. A clear explanation of this result, as of the presence of an energy threshold for the observed rise in the transverse momenta, can be obtained from Fig. 13 of Ref. 52. One should expect a decrease of the average product of the deviation of the hadron from the shower axis  $R$  and the hadron energy  $E$  with increase of the intensity of the shower (i.e., the energy of the primary particle). In fact, hadrons of a given energy are produced at greater depths in the atmosphere, the higher is the energy of the primary particle. In contrast to the predicted dependence, measurements show a rise of the product  $\langle ER \rangle$  beginning with a primary-particle energy  $\sim 100$  TeV/nucleon.

In addition it must be noted that it would be premature to conclude from Fig. 12 that there is an ever increasing value of the average transverse momentum with increase of the primary energy, since the complex composition of the primary cosmic radiation broadens the region of the threshold effects in which an ever increasing fraction of the primary particles which have produced a shower with a given number of electrons have an energy  $\geq 100$  TeV/ $c$  nucleon.

The distribution of transverse momenta has been investigated more directly by means of nuclear emulsion and x-ray emulsion chambers. In Fig. 14 we have given the results of measurements in nuclear emulsions for interacting-hadron energies  $\sim 20$  TeV (Ref. 53) and in x-ray emulsion chambers<sup>1</sup> for families of  $\gamma$  rays with a primary energy  $\sim 100$  TeV. All distributions of transverse momenta have been multiplied by  $\exp(6p_\perp)$ , where  $p_\perp$  is the value of the transverse momentum. The similar curves, which are  $\sim p_\perp \exp(-5p_\perp)$ , correspond to the distribution of transverse momenta at an incident-proton energy of  $\sim 0.2$  TeV obtained by means of a bubble chamber.<sup>54</sup> A comparison shows that in the range of transverse momenta from 0.2 to 2 GeV/ $c$  for a change of the primary energy from the accelerator region  $\sim 0.2$  TeV to energies  $\sim 100$  TeV no significant changes are observed in the distribution of transverse momenta of the secondary pions. Analysis of the data of the Pamir experiment led to the conclusion that for high energies ( $\sim 1000$  TeV) no appreciable rise in the transverse momenta of the  $\gamma$  rays is observed.<sup>55</sup>

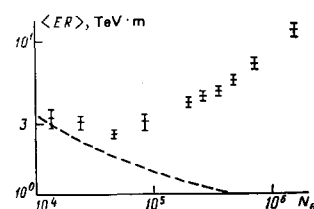


FIG. 13. Average product  $\langle ER \rangle$  as a function of the number of electrons  $N_e$  in the shower. Here  $E$  is the energy of the hadron and  $R$  is its distance from the shower axis. The curve shows the expected dependence. The primary energy of the particle which produced the shower is  $E_0 \approx 2 \cdot 10^3 N_e$  TeV.

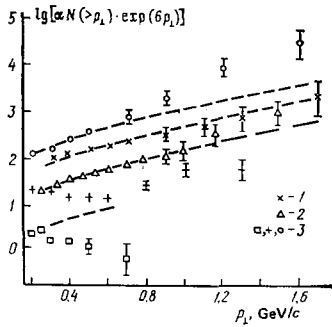


FIG. 14. Distributions of transverse momenta for incident-hadron energies  $E_0 \approx 20$  TeV (1) and  $E_0 \approx 100$  TeV (2) without additional selection. Data with additional selection criteria corresponding to H-quanta, SH-quanta, and UH-quanta for  $E_0 \approx 100$  TeV are shown by (3) in the same sequence.

We might discuss the contradiction between the results of study of secondary-hadron transverse momenta by the method of extensive air showers and the results of x-ray emulsion chambers, if the x-ray emulsion chambers themselves did not give indisputable cases of the recording of multiple-production events with large transverse momenta of the secondary particles. The best case of the class of events which are called centaurs has a generation altitude of  $50 \pm 15$  m above the level of observation. The average transverse momentum of the hadrons (presumably nucleon-antinucleon pairs) is estimated<sup>1</sup> as  $\langle p_{\perp} \rangle = 0.35/K$  GeV/c, where  $K \approx 0.2-0.33$ . In the exposure of an x-ray emulsion chamber on Mount Fuji an event was recorded with a group of hadrons with total energy  $\geq 4 \cdot 10^3$  TeV (Titan).<sup>56</sup> The transverse momenta between the hadrons of the group amount to 1.7–2 GeV/c. The French-Japanese group of investigators of inelastic hadron collisions by means of x-ray emulsion chambers observed in an aeroplane flight a case of hadron interaction in the construction materials of the aeroplane at a distance of 2.2 m from the chamber.<sup>57</sup> Here the secondary particles are grouped into four groups. The distance between them corresponds to transverse momenta greater than 1 GeV/c. In the experiments on Chacaltaya among the set of  $\gamma$ -ray families cases are identified of pairs of genetically related families, so-called twin (geminion) and binocular events.<sup>58</sup> The transverse momentum between the jets responsible for such events exceeds 10 GeV/c. Analysis of the azimuthal distribution in  $\gamma$ -ray families on the basis of the data of the Pamir experiment shows a jet structure in part of the families with values of transverse momentum between jets of several GeV/c.<sup>59</sup>

The enumeration of all these separate and greatly varied cases of detection of groups of  $\gamma$  rays and hadrons with large transverse momenta could be continued. Their combined frequency of appearance exceeds 10% of the effective cross section for inelastic collision of hadrons with nuclei of air atoms. Whether this is sufficient for interpretation of the experimental data<sup>45, 52</sup> on large transverse momenta of hadrons in extensive air showers is hard to say without special calculations.

At the present time all experiments intended for study of large transverse momenta confirm the existence of

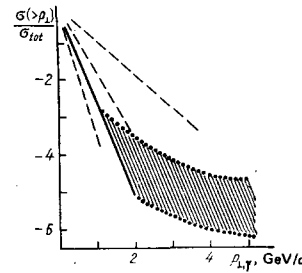


FIG. 15. Distribution of transverse momenta of  $\gamma$  rays. Solid straight line:  $\sim e^{-6 p_{\perp}}$ ; dashed straight lines: grouping according to H-, SH-, and UH-quanta ( $\sim e^{-8 p_{\perp}}$ ,  $\sim e^{-4 p_{\perp}}$  and  $\sim e^{-2 p_{\perp}}$ ); the dotted curve shows a distribution of the form  $\sim p_{\perp}^{-4}$ .

cases with high momenta (more than 1 GeV/c and even tens of GeV/c). The distribution of transverse momenta in magnitude can be described<sup>60</sup> as  $\sim p_{\perp}^{-4}$ . Disagreements in the conclusions<sup>43</sup> of different measurements begin in the attempts to estimate the cross section for generation of particles with large transverse momenta. While the exponential distribution observed at transverse momenta  $< 1$  GeV/c for pions gradually goes over at high momenta to a power law  $\sim p_{\perp}^{-4}$ , the absolute and relative (as in Fig. 15) effective cross sections for large values of transverse momenta are small. In this case the average value of the transverse momentum is determined by the exponential part of the distribution. However, it is impossible to explain by these means either the experimental data of Refs. 45 and 52 or the events with high transverse momenta observed in x-ray emulsion chambers.<sup>56-59</sup> Evidently the formation of hadrons with high transverse momenta must be related to individual cases of the generation of energetically distinguished particles with large deviations from the direction of the primary particle, jets, and other special events.

## 7. H-QUANTA, SH-QUANTA, CENTAURS, GEMINIONS, ETC.

The analysis of a substantial part of the families of cosmic-ray  $\gamma$  rays and hadrons recorded in x-ray emulsion chambers is carried out from the point of view of the hypothesis of H-quanta, and in discussing the experimental data on multiple production at incident-hadron energies above 100 TeV it is impossible to avoid mentioning this hypothesis. The idea of H-quanta was introduced by Hasegawa<sup>61</sup> and stood for some intermediate state in the multiple production of hadrons. The distinction of H-quanta from a fireball is that a definite mass was not assigned to fireballs. The confirmation of a fixed mass of the H-quantum was perceived in the proportionality between  $\gamma_s$ , which is determined from the relation  $\ln \gamma_s = -\langle \ln \text{tg } \theta_i \rangle$ , and the total energy of the  $\gamma$  rays in a family  $\sum E_i$  (Fig. 16); here  $\theta_i$  is the angle between the direction of emission of the  $i$ -th  $\gamma$  ray and the energy-weighted direction of all  $\gamma$  rays of the family. If we assume that all observed  $\gamma$  rays are produced in a single cluster, then the mass of the cluster which has gone into  $\gamma$  rays is  $\sum E_i / \gamma_s = 1.3$  GeV/c<sup>2</sup>. The total mass should be three times larger if we assume equally probable production of pions with different

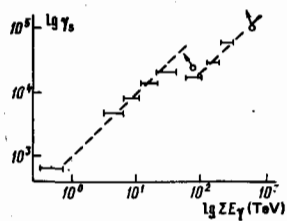


FIG. 16. Lorentz factor  $\gamma_s$  of the center of symmetric emission of a  $\gamma$ -ray family as a function of the total  $\gamma$ -ray energy.<sup>64</sup> (The arrows show the shift of the data on individual families if it is assumed that the  $\gamma$  rays are produced in two clusters.)

charges. However, the fluctuations in the distribution of energy between charged and neutral pions and the sample of events for the decreasing energy spectrum of cosmic rays reduce the mass to 2.6 GeV/c<sup>2</sup>.<sup>62</sup> The greatest popularity of the hypothesis of H-quanta in application to analysis of data on families of  $\gamma$  rays in x-ray films occurred in the period when, as statistics were accumulated, data appeared on  $\gamma$ -ray families of higher multiplicity and higher total energy. These families fell outside the previously established proportionality between  $\gamma_s$  and  $\Sigma E_i$  and in this way corresponded to clusters of larger mass (SH-quanta). The  $\gamma$ -ray family of very high energy "Andromeda" observed at that same time<sup>63</sup> permitted one to suppose that even heavier clusters existed, UH-quanta. In the final analysis the following picture was drawn: H-quanta, SH-quanta, and UH-quanta with masses 2.6, 30, and 200 GeV/c<sup>2</sup> are effectively produced in the corresponding intervals of the colliding-hadron energy, and the transverse momenta of the  $\gamma$  rays in these classes of families are distributed exponentially [ $\sim \exp(-p_\perp/p_0)$ ] with the respective values of the parameter  $p_0$  125, 250, and 500 GeV/c.

In order to be convinced of the reality of this picture, it is necessary to establish the quantized nature of the mass values of the H-, SH-, and UH-quanta with a sample of events independent of the transverse-momentum values of the  $\gamma$  rays in the family. The mass of UH-quanta is undetermined, since the few events assigned to this class are extremely diverse. The experimentally obtained distribution in mass (in terms of quanta  $M_\gamma$ ) for H- and SH-quanta is shown in Fig. 17. The most important detail of this distribution is the small number of events with mass 3–4 GeV/c<sup>2</sup>. However, neither the statistical reliability of this distribution nor the accuracy in determination of the cluster

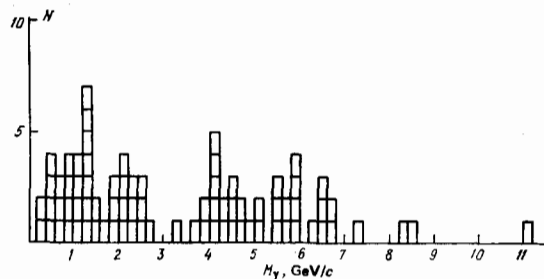


FIG. 17. Distribution in mass (in terms of  $\gamma$ -quanta) of clusters from Ref. 1.

mass in individual events permits the discreteness of the mass values of the H-, SH-, and UH-quanta to be considered proved. Furthermore, frequently events assigned on the basis of their mass to SH-quanta, when analyzed by the method of Duller and Walker diagrams, would be assigned to events with observation of two clusters, rather than one.<sup>64</sup>

The grouping in mass of analyzed jets of multiple production was carried out at first on the basis of the ratio between the Lorentz factor of the center of symmetry and the total energy of the  $\gamma$  rays. Later the Shibata relations<sup>75</sup> were used, which took into account more completely the entire existing experimental information. At the present time the Japanese-Brazilian Collaboration is using a more convenient separation of events into H-, SH-, and UH-quanta (Fig. 18). However, in the right-hand part of the diagram where the data of different families are best distinguished, the ordinates are proportional to the product  $n \langle p_\perp \rangle$  where  $n$  is the number of  $\gamma$  rays in the family, and after grouping on the basis of this characteristic, the difference of the distribution of the momenta  $p_\perp$  in H-, SH-, and UH-quanta cannot be an independent confirmation of the reality of such objects, since it reflects the criteria of the sampling. Incidentally, the distributions of the transverse momenta in Fig. 14 for H-, SH-, and UH-quanta are characteristic of the fact that the greatest difference from the general averaged distribution of transverse momenta is not for UH-quanta, but for H-quanta with smaller than average transverse momenta. Perhaps the segregation of H-quanta picks out events of the diffraction production of pions.

At the same time, an individual analysis of multiple-production events recorded in x-ray emulsion chambers has permitted a number of additional interesting cases of multiple production to be observed at incident-hadron energies  $\sim 1000$  TeV. The so-called centaurs have become the best known events. A diagram of the first and most effective of the observed centaurs is shown in Fig. 19. The main feature of centaurs is the absence, in the hadron jet arriving from the atmosphere at the x-ray emulsion chamber, of neutral pions in the proportion necessary for multiple-production processes. Several such events have been found (Table II) and this permits the statement that the features of centaurs cannot be explained by fluctuations of ordinary multiple production of hadrons. The absence of  $\pi^0$  mesons in the hadron jet strikingly separates these events from the background of ordinary fluctuations of the composition

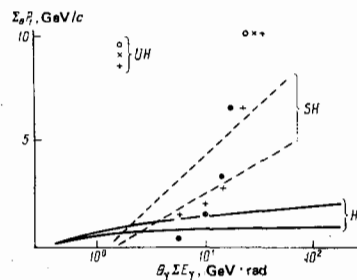


FIG. 18. Means of grouping of  $\gamma$ -ray families according to the classes H-quanta, SH-quanta, and UH-quanta in Ref. 1.

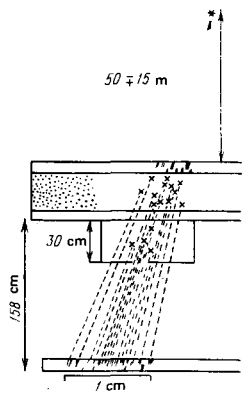


FIG. 19. Centaur I, produced at a height  $\sim 50$  m above the x-ray emulsion chamber and containing 49 observed hadrons which undergo collisions, mainly with light nuclei of the carbon target and of the wood beam under the upper block.<sup>1</sup>

of the secondary particles; in analysis of the centaur (Fig. 19) the order of assembly and disassembly of the x-ray emulsion chamber was specially checked to exclude the suggestion that the recorded jet entered the x-ray emulsion chamber during the assembly of the apparatus. In addition, the presence in the upper block of cascades which are continued in the lower block argues against this assumption.

Table I lists the characteristics of centaurs on the basis of the experiments.<sup>1</sup> The numbering of the events corresponds to all publications of the data on these centaurs. The number in parentheses indicated the number of the x-ray emulsion chamber in the exposures at Chacaltaya (5220 m above sea level). All electron-photon cascades, jets produced in the lead of the lower chamber (see Fig. 19), in the carbon target, and in the wood construction under it or in the lead of the upper chamber at a depth of more than 10 cascade units, and also jets beginning in the upper chamber but having two maxima in their development with depth, were considered to be hadrons. The cascades associated with electrons and  $\gamma$  rays include both explicit cases of showers from the atmosphere and a significant portion of the jets in the upper chamber, of the number which are insufficiently determined when the jets are not associated with a hadron interaction in the lead of the upper chamber.

The height of formation of the centaur can be determined from the divergence angle of the jet only for event No. I(15). In the remaining events it has been estimated from the lateral distribution of the jets on the assumption of a single transverse-momentum distribution for all centaurs, which was found for centaur I(15) to have an average value  $\langle p_{\perp} \rangle = 1.7 \pm 0.7$  GeV/c. The expected number of  $\gamma$  rays (electrons) from secondary interactions in the atmosphere is estimated on the assumption of the usual observed pattern of production of  $\gamma$ -ray families by hadrons and also on the basis of the height and the number of hadrons in a given centaur. The difference between this estimate and the observed number of  $\gamma$  rays from the atmosphere gives the number of  $\gamma$  rays from  $\pi^0$  mesons which have arisen in the initial event of formation of the centaur above the ap-

paratus. The total number of hadrons in the centaur production event is estimated on the basis of the observed number of jets in the apparatus with allowance for the efficiency of detection of hadrons in the x-ray emulsion chamber and the probability of their interaction in the atmosphere in the path from the production event to the level of observation. The total energy of the interaction is determined from the total number of hadrons and the observed energy spectrum of the hadrons in the centaur.

The authors of studies of centaurs<sup>1,62,65</sup> consider it possible to interpret these events as heavy fireballs with a mass  $\sim 230$  GeV/c<sup>2</sup> which decay into baryons and antibaryons. Here the closeness of the masses of the centaurs and the UH-quanta permits the authors of this interpretation to envisage a parallelism in these phenomena and to speak of a difference only in the decay modes: ordinary pion emission of a fireball in the case of the UH-quantum and baryon-antibaryon emission in the centaurs. With this approach the SH-quanta are placed in correspondence with the so-called minicentaurs, which differ from centaurs in a smaller number of hadrons and a lower total energy. However, the identification of minicentaurs in a background of fluctuations in the composition of individual  $\gamma$ -ray and hadron families is less convincing.

The experimental fact of generation of large groups of hadrons with an extremely insignificant fraction of  $\gamma$  rays ( $\pi^0$  mesons) is very hard to doubt, especially since such anomalous groups of hadrons have been observed, although with a lower frequency, also in other experiments.

The question of the interpretation of centaurs is extremely ambiguous. The parallelism between UH-quanta and centaurs we shall put aside, since in reality there is still no confidence in H-, SH-, and UH-quanta. The identification of centaurs with heavy fireballs is based exclusively on the analysis of the centaur I(15), which is so far the only event in which the height of generation of the hadrons can be determined without assumptions regarding the characteristics of the production event, resting only on the lateral separation of the observed hadrons. The two jets of centaur I(15) are easily followed into the upper and lower blocks of the x-ray emulsion chamber, and here the distance between the spots in the lower block is greater by  $0.25 \pm 0.05$  mm than in the upper block. With allowance for the distances between the blocks and between the jets composing the pair, the height of the point of production of this pair is found to be  $50 \pm 15$  m. The separations of the pairs of jets in the lower block of the x-ray emulsion chamber is statistically better described but less accurately measured. The distribution of the heights of generation  $h$  is given in Fig. 20 with allowance for the accuracy in determination of this height  $\Delta h$ . The height  $50 \pm 15$  m is represented only weakly in this distribution: 9 pairs of jets correspond to a production height below 25 m and 7—above 90 m. Thus, the assumption that the hadrons observed in the centaur I event are produced in an isotropically emitted fireball at a height  $\sim 50$  m agrees poorly with the distribution in height of the points of convergence of the hadron pairs

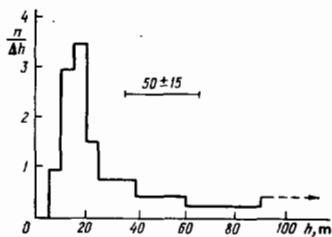


FIG. 20. Distribution of heights of points of geometrical convergence of pairs of cascade jets, taken as the point of production, from the data of the lower block of the x-ray emulsion chambers for the centaur I.  $\Delta h$  is the error in determination from a pair of cascades observed both in the upper block and in the lower block of the chambers.

(see Fig. 20). Also in disagreement with this assumption are the values of the transverse momenta of the hadrons in the central and peripheral parts of the hadron family. If all or most of the hadrons of the family of centaur I were generated in a single interaction from an isotropically decaying cluster at a height of 50 m, then the average values of the transverse momenta near the center of the family and the periphery would be identical. Experimentally the hadrons closer to the center have on the average a factor of two smaller transverse momentum than the hadrons removed from the center of the family. This difference means either a so far unobserved anisotropy of emission in the rest system of the cluster with a preference in momentum for particles emitted at large angles to the direction of the colliding particles, or generation of the hadrons at different heights.

In concluding our discussion of the question of centaurs it is necessary to mention that the arguments given above against the interpretation of centaurs as special decays of heavy fireballs (UH-quanta) further emphasize the singularity of the observed phenomenon. The repeated nature of the generation of a group of hadrons of unusual composition (without  $\pi^0$  mesons) substantially decreases the probability that such groups are produced by means of multiple production in hadron inelastic collisions. It is more likely that centaurs are the results of a cascade of decays into baryons and antibaryons of heavy particles with lifetimes  $10^{-11}$ – $10^{-12}$  sec.

Another type of special event observed in x-ray emulsion chambers is the so-called binocular event.<sup>66</sup> Binocular events are characterized by the existence of

TABLE II. Number of hadrons observed in XEC (x-ray emulsion chamber).

Designation of the event	I (15)	II (17)	III (17)	IV (17)	V (16)
Number of hadrons observed in XEC (x-ray emulsion chamber)	49	32	37	38	31
Number of cascades associated with electrons and $\gamma$ rays above the XEC	1	0	17	51	31
Height of generation event, m	50	80	230	500	400
Expected number of $\gamma$ rays from secondary interactions in the atmosphere	4	13	30	47	32
Number of $\gamma$ rays associated with the initial production of the centaur	—	—	—	5	—
Number of hadrons in the centaur production event	74	71	76	90	63
Total estimated energy, TeV	330	370	350	340	350
Energy measured in the XEC, TeV	270	200	270	290	280

two ordinary families of  $\gamma$  rays separated by a distance of  $\sim 20$  cm with a spread of the  $\gamma$  rays inside each family in the range 1–3 cm. The general pattern of the events recalls jets with large transverse momenta<sup>67</sup> due to hard scattering of the quarks of the colliding hadrons. However, the direct transfer of accelerator data on such jets to this phenomenon cannot explain any appreciable fraction of the binocular events.<sup>1</sup> This circumstance stimulates the authors of Refs. 1 and 66 in their search for new interpretations of binocular events to propose the hypothesis of "twins" (geminions), according to which in interactions of hadrons at the energies considered here some "double" particle with mass 16–24  $\text{GeV}/c^2$  is produced with a probability  $\sim 10\%$  and decays with a short lifetime into baryons with a high decay energy, which gives large transverse momenta ( $\sim 10 \text{ GeV}/c$ ) of the baryons. Here the term baryon is used to exclude the possibility of a fast electromagnetic decay of the hadrons of a pair. The baryons, undergoing inelastic collisions with nuclei of air atoms at a height  $\leq 500$  m above the apparatus, form ordinary  $\gamma$ -ray families. These values of the parameters of the twin hypothesis correspond to the experimentally observed energies of the families and the distances between families. An indication that single hadrons are produced in the decay of the initial particle lies in the individual cases in which a single jet turns out to be paired with a family of  $\gamma$  rays. The case of production of baryon-twins in the roof above the x-ray emulsion chamber also serves as an indication of this (Fig. 21).

On the whole the analysis of x-ray emulsion data on the assumption of production of secondary hadrons in fireball-clusters puts into schematic form an exclusive grouping of the events. By this means the authors of Ref. 1 group almost all hadron multiple-production events in the super-accelerator energy region.

Small jets—Mirim as they are called in Ref. 65, or H-quanta—reflect the extrapolation to the high-energy region of approximate scale-invariant characteristics of the fragmentation part of the secondary hadrons observed in accelerators. The masses of the H-quanta are 2–3  $\text{GeV}/c^2$ , and the secondary particles are pions.

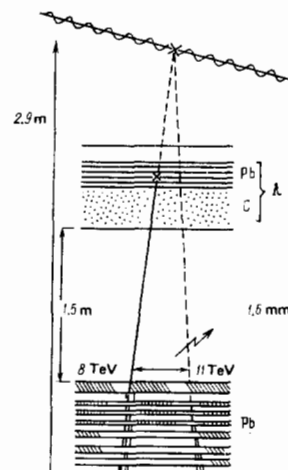


FIG. 21. The binocular event Castor and Pollux from Ref. 66.

Large jets, Acu in the terminology of Ref. 65 or SH-quanta, are characteristic only of energies above a few tens of TeV, and their appearance reflects the violation of scaling in the fragmentation part of the inclusive spectrum of secondary hadrons. The mass of the SH-quanta is 15–30 GeV/c<sup>2</sup> and they decay into H-quanta. Minicentaurs and geminions<sup>66</sup> have the same mass but decay into many baryons, respectively.

Finally, the very large jets (Guacu of Ref. or UH-quanta), like centaurs, have a mass 100–300 GeV/c<sup>2</sup>. The UH-quanta decay into H-quanta, and the centaurs into baryons.

This is the hypothetical picture of multiple processes in the energy region 10–1000 TeV given by the physicists of the Japanese-Brazilian collaboration.<sup>1</sup> Both the weak aspects of the experimental basis and the arbitrariness in its construction, as well as the difficulty in reconciling it with the details of experimental data which it was not intended to explain, have been noted in the course of describing the results of the work.

## 8. SOME RESULTS OF THE PAMIR EXPERIMENT

The separate description of the results obtained by this collaboration<sup>1)</sup> is due to the fact that this work utilizes a fundamentally different approach to analysis of the experimental data, different both from that set forth in the previous section, and from practically all other studies with x-ray emulsion chambers. Here in the primary analysis of the experimental data and their statistical grouping, no *a priori* assumptions are made regarding the nature of multiple-production processes. Such assumptions are made in the calculations which model the experiment, and the conclusions regarding the real physical processes in inelastic collisions of hadrons are based on comparison of the calculations with the experiment. This approach to the analysis of experimental data has already been described in discussion of the results of study of the fluxes of the various components of cosmic rays in the depth of the atmosphere for the energy interval 1–100 TeV. Here we shall give data on families of  $\gamma$  rays and hadrons in the energy region 30–10<sup>4</sup> TeV.

In Table III we compare the observed and calculated intensities of  $\gamma$ -ray families with a total energy of the  $\gamma$  rays observed in the x-ray film  $\sum E_\gamma \geq 30$  TeV at an atmospheric depth of 596 g/cm<sup>2</sup>. The experimental value of the flux was obtained on the basis of Refs. 68–70. The calculations according to the scaling and quasiscaling models<sup>28</sup> take into account in the former case a simple extrapolation from the accelerator data in ac-

1) The Pamir experiment is being carried out by a collaboration of several institutes: Physics Institute of the Academy of Sciences of the USSR, Nuclear Research Institute of the Academy of Sciences of the USSR, Nuclear Physics Institute of Moscow State University, Institute of High Energy Physics of the Kazakh Academy of Sciences, Physics Institute of the Georgian Academy of Sciences, Physico-technical Institute of the Tadzhik Academy of Sciences, Physico-technical Institute of the Uzbek Academy of Sciences, Physics Institute of the University of Lodz (Poland), and Nuclear Physics Institute at Krakow (Poland).

TABLE III. Calculation on the basis of models of the interaction event.

Calculation on the basis of models of the interaction event			Experiment, m <sup>-2</sup> y <sup>-1</sup> sr <sup>-1</sup>
Scaling	Quasiscaling	High multiplicity	
19	7.4	2.2	2.4 <sup>+1.6</sup> <sub>-0.6</sub>

cordance with the laws of Feynman scaling, and in the latter case the entire rise of the effective cross section for inelastic collisions is assigned to pionization processes. A model with high multiplicity  $n \sim \sqrt{E}$  and a constant effective cross section has been considered in Ref. 71. Comparison of theory and experiment shows that it is insufficient to take into account scaling violation only in the pionization part of the inclusive spectrum of secondary hadrons if one is to attempt to explain the observed intensity of  $\gamma$ -ray families.

The change of the secondary-hadron energy spectrum in the fragmentation part can be seen both in the energy distributions and in the number of high-energy  $\gamma$  rays in a family. To distinguish the most energetic portion of the  $\gamma$  rays by a means which does not depend on the energy of the family, we considered  $\gamma$  rays with a relative detection threshold  $f' = E_\gamma / \sum E'_i \geq 0.04$ . Only  $\gamma$  rays with  $f' \geq 0.04$  are included in the sum over  $E'_i$ . In Fig. 22 distributions in  $f'$  and in the number  $n'_\gamma$  of such  $\gamma$  rays in families with various total energies of all  $\gamma$  rays are compared with the values expected on the assumption of scaling in the fragmentation part of the inclusive spectrum.<sup>72</sup> In Table IV we have given a comparison of  $\langle n'_\gamma \rangle$  for  $\gamma$ -ray families of various energies with values calculated for scaling and for the high-multiplicity model.<sup>73</sup>

Here it should be noted that breaking up the experimental data into various groups  $\sum E_\gamma$  does not greatly change the energy of the hadrons which generate these families, as a result of the very wide representation of different energies of the primary particles responsible for a family of  $\gamma$  rays of a given energy.

The conclusion which follows from the analysis presented of the experimental data of the Pamir Collabora-

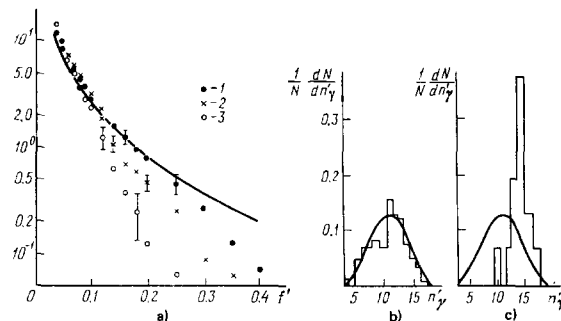


FIG. 22. a) Number of  $\gamma$  rays with  $f'$  greater than a given value for families of  $\gamma$  rays with total energy 50–100 TeV (1), 100–200 TeV (2), and 200–400 TeV (3) (the curve shows the expected distribution on the assumption of scaling in the fragmentation part of the inclusive spectrum); b and c) distributions in  $n'_\gamma$  for families with a total  $\gamma$ -ray energy 50–100 TeV and 200–400 TeV, respectively (the curves are the distribution expected for scaling).

TABLE IV.

E, TeV	$\langle n_\gamma \rangle$		
	Scaling	High multiplicity	Experiment
50-100	10.8±0.4	13.2±0.4	10.5±0.3
100-200	10.5±0.6	13.6±0.4	12.0±0.3
200-400	10.8±0.7	14.3±0.5	14.0±0.4

tion, that there is a high multiplicity of secondary particles and a large dissipation of energy in inelastic collisions of nucleons with nuclei of air atoms at primary energies  $\sim 10^3$  TeV, was drawn previously on the basis of an analysis of the development of extensive air showers in the upper part of the atmosphere.<sup>74</sup>

However, before turning from the Pamir experiment to the development of extensive air showers in the atmosphere, it is necessary to consider an extremely exotic case of incidence of a family of  $\gamma$  rays and hadrons on the x-ray emulsion chamber of the Pamir experiment, which contained both blocks for detection of  $\gamma$  rays from the atmosphere and blocks under layers of carbon for measurement of the hadron flux (see Fig. 1). Among families of  $\gamma$  rays with a primary energy above  $10^3$  TeV one encounters families in which the entire central part of the family of area several square millimeters or more has an increased background of darkening.<sup>64,75,76</sup> There is as yet no unique interpretation of such events, especially since such a "halo" can occur also with scale-invariant characteristics of the multiple production of hadrons in inelastic collisions of cosmic-ray primary protons at energies of  $10^4$  TeV.<sup>77</sup> In the latter case the observed number of events with a halo amounts to 5% of the expected number, and it is not clear whether one can consider this fraction as the fraction of scaling processes of secondary-particle production.<sup>76</sup> The exotic nature of the Tat'yana event<sup>78</sup> lies in the fact that in a given family with a  $\gamma$ -ray energy above  $10^3$  TeV and total energy above  $10^4$  TeV the halo in an area of  $\sim 8$  mm is observed at all depths of the hadronic block without appreciable absorption over a length of 2.5 hadron interaction ranges or 55 electromagnetic cascade units.

The hopes for progress in analysis of the data of the Pamir experiment are placed on a comparison of  $\gamma$  rays

TABLE V.

	$\langle n_\gamma \rangle$	$\langle n_h \rangle$	$\langle \frac{n_h}{n_\gamma} \rangle$	$\langle \frac{\sum E_h^\gamma}{\sum E_\gamma} \rangle$
Experiment	9.2±1.6 $\sigma = 5.6$	4.3±1 $\sigma = 4.5$	0.56±0.08 $\sigma = 0.36$	0.81±0.22 $\sigma = 1.0$
Model	7.8±0.2 $\sigma = 5.3$	3.0±0.1 $\sigma = 2.6$	0.44±0.01 $\sigma = 0.33$	0.93±0.05 $\sigma = 1.24$
	$\langle R_\gamma \rangle$	$\langle R_h \rangle$	$\langle E_\gamma R_\gamma \rangle$	$\langle E_h^{(\gamma)} R_h \rangle$
Experiment	30.5±4 $\sigma = 13$	94±15 $\sigma = 60$	234±25 $\sigma = 112$	924±260 $\sigma = 1180$
Model	22.4±1.0 $\sigma = 24$	64±5 $\sigma = 180$	170±8 $\sigma = 200$	950±90 $\sigma = 2200$

and hadrons in the same families. This work is only beginning. In Table V data on 20 families of  $\gamma$  rays and hadrons found in an x-ray emulsion chamber with a uniform lead absorber are compared with the expected characteristics calculated on the assumption of scaling in the fragmentation portion of the inclusive spectrum and violation of scaling in the pionization region.<sup>79</sup> The photon-hadron families were selected on the basis of  $\gamma$  rays with total energy  $E_\gamma \geq 30$  TeV and with a number of  $\gamma$  rays  $n_\gamma \geq 3$  at energies  $E_\gamma \geq 4$  TeV within a radius  $R_\gamma = 15$  cm. The search for hadrons accompanying the  $\gamma$  rays was carried out to distances  $R_h = 30$  cm from the center of the  $\gamma$ -ray family. Hadrons with energy above  $E_h^{(\gamma)} \geq 4$  TeV were taken into account ( $E_h^{(\gamma)}$  is the hadron energy transmitted to  $\gamma$  rays). Although the average values of the characteristics of the photon-hadron families in Table V do not reveal explicit differences, one can see already from these preliminary data a lack of correspondence of the experiment to the model on which the calculation was based. This may consist of the significantly greater spread in the number of hadrons ( $\sigma$  amounts to 4.5 in the number of hadrons in the experiment, compared to  $\sigma = 2.6$  according to the calculation), as in the spatial characteristics of the family.

9. DEVELOPMENT OF EXTENSIVE AIR SHOWERS IN THE ATMOSPHERE

Protons and nuclei of the primary cosmic radiation at energies above 100 TeV produce hadronic cascades in passing through the Earth's atmosphere. A large part of the energy of these cascades, as a consequence of the production of  $\pi^0$  mesons among the secondary particles, is transferred to the electron-photon component of extensive air showers. On the other hand, the rapid development of the electron-photon component of the shower and the depth of the maximum of the cascade development in the atmosphere are uniquely related to the energy spectrum of the  $\gamma$  rays (or  $\pi^0$  mesons) at the beginning of the development of the hadronic cascade and in this way to the characteristics of the multiple-production process in inelastic collisions of the primary nucleons with nuclei of air atoms. For just this reason the observation of a high intensity of extensive air showers at high altitudes<sup>74</sup> was immediately associated with a high dissipation of energy in the first nucleon-nucleus collision at the edge of the atmosphere. In Fig. 23 we have shown these experimental data to-

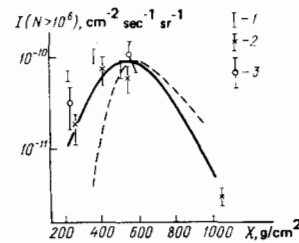


FIG. 23. Intensity of extensive air showers in the upper part of the atmosphere: 1—experiment in aeroplane,<sup>74</sup> 2—measurements in balloons in 1976,<sup>80</sup> 3—measurements in balloons in 1973.<sup>80</sup> Solid curve—expected intensity for a multiplicity  $n \sim E_0^{0.5}$ ; dashed curve—for  $n \sim \ln E_0$ .

gether with contemporary data on the intensity of extensive air showers with a number of particles  $N > 10^6$  at high altitudes.<sup>80</sup> The intensity of showers at sea level agrees satisfactorily with measurements in the large experimental installations, which have a high accuracy in detection of each shower. Observations of extensive air showers at high altitudes are greatly complicated by the limitation of the possible size of the apparatus carried in an aeroplane<sup>74</sup> or an automatic balloon.<sup>80</sup> As a consequence there are substantial uncertainties in the lateral distribution of the particles in the shower, and in the early experiments also in the zenith angle at which the shower is observed. However, the differences in the intensity in the experiment and in calculations (on assumptions similar in their parameters to a scaling extrapolation of the accelerator data) are so great that in its qualitative aspect the conclusion that there is a high multiplicity in events at a primary-nucleon energy  $\sim 10^3$  TeV is convincing.

The dependence of the number of particles in the shower on the depth of measurement in the atmosphere can be traced in more detail on the basis of the experiments<sup>81</sup> carried out at the Chacaltaya high altitude installation. The different depth of measurement in the atmosphere for a fixed location of the measuring apparatus is achieved by selection of extensive air showers with identical intensity at different zenith angles. If fluctuations are neglected, this is equivalent to selection of extensive air showers with a given primary energy. In Fig. 24 we have shown data obtained in this way for the number of electrons  $N_e$  as a function of the depth of measurement in the atmosphere for showers with intensities of  $10^{-8}$ ,  $10^{-9}$ ,  $10^{-10}$ , and  $10^{-11}$   $\text{m}^{-2}\text{sec}^{-1}\text{sr}^{-1}$ . For comparison in the same figure we have given other experimental results obtained by establishing the number of electrons in the shower at various heights on the basis of the lateral distribution of the Cherenkov flashes at sea level on passage of the shower through the atmosphere.<sup>82</sup>

For analysis of the experimental data, calculations<sup>23</sup> are used in which the rise of the effective cross section for inelastic collisions with increasing energy of the incident particle is taken into account (Fig. 4), and three types of dependence of the secondary-particle multipli-

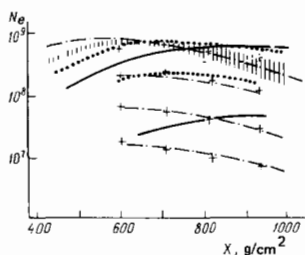


FIG. 24. Number of electrons in extensive air showers of a given primary energy as a function of depth in the atmosphere. The experimental data of Ref. 1 are given by the crosses. The cross-hatched band is the behavior with altitude established from the lateral distribution of the Cherenkov flash at sea level.<sup>82</sup> Expected dependences: solid curves—for a multiplicity  $n \sim \ln E$ , dashed curve—for  $n \sim E^{1/4}$ , dot-dash—for  $n \sim E^{1/2}$ .

city on the energy of interaction were tried:  $n \sim \ln E$ ,  $n \sim E^{1/4}$ , and  $n \sim E^{1/2}$ . In inelastic collisions at energies below 3 TeV, characteristics were taken which correspond to measurements in accelerators. The calculations of Ref. 23 were carried out for primary protons. Since the usual composition of the primary cosmic radiation (see Table 1) on averaging has an average number of nucleons per particle  $\langle A \rangle \approx 10$ , the calculated dependences of the number of particles in a shower at various depths in the atmosphere were recalculated for the case of a given energy of a primary nucleus with  $A = 10$ . The conversion was made on the basis of the model of superposition, in which it is assumed that a shower from a primary nucleus  $A$  with energy  $E$  is equivalent to the sum of  $A$  showers from primary protons with energy  $E/A$ . As can be seen from Fig. 24, the behavior with altitude of the number of electrons in a shower for primary energies  $5 \cdot 10^3 - 10^5$  TeV is inconsistent with a logarithmic (scaling) dependence of the secondary-hadron multiplicity on the incident-particle energy and can be reconciled with a dependence of the type  $n_s = 0.13E^{1/2} + 7$ . For energies of the primary nuclei  $\geq 10^5$  TeV the observed location of the maximum of the shower development in the atmosphere corresponds to a smaller multiplicity than is given by this formula. In addition, it must be kept in mind that the height of the maximum of development of the shower will depend also on the composition of the secondary particles. This question will be discussed in the next section.

The altitude dependence of the number of muons in a shower, which has been studied, in particular, in the same experiment,<sup>81</sup> in comparison with the theoretical calculations turns out to be closer to the variants with a high multiplicity of secondary particles in the inelastic collision of hadrons with nuclei of air atoms (Fig. 25).

The experimental dependences shown in Fig. 25 for the number of electrons and muons as a function of the

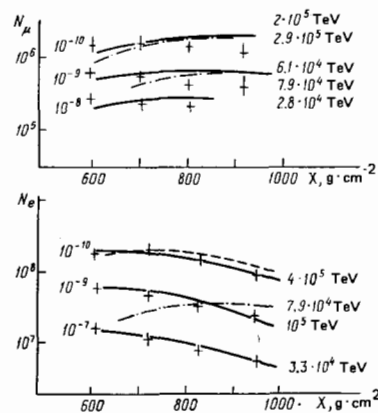


FIG. 25. Number of muons  $N_\mu$  and number of electrons  $N_e$  in extensive air showers as a function of depth in the atmosphere. The numbers at the left of the experimental data indicate the frequency of occurrence of such showers. The curves show the expected dependence for various multiplicities of hadrons in the event: solid curves— $n \sim E^{1/2}$ , dashed curves— $n \sim E^{1/4}$ , dot-dash— $n \sim \ln E$ . The numbers at the right of the curves indicate the energy of the primary nucleus if it is assumed that it has  $A = 10$ .

depth in the atmosphere correspond to three primary-particle energies which are identical both in measurements of the muon flux and in determination of the number of electrons, because showers with an identical frequency of appearance were selected. However, the calculated dependences, which give the experimentally observable values of  $N_e$  and  $N_\mu$ , differ in primary energy by 15–50%. It was noted long ago that there is a preferential transfer of energy to the electron-photon component of a shower in comparison with that expected for the ratio known from the accelerator energy region of  $\pi^0$ ,  $\pi^\pm$ , and  $K$  mesons generated in hadron interactions. This fact, which has arbitrarily been called "gammanization",<sup>43</sup> signifies that there are some additional channels of energy transfer from the primary nucleons to the electron-photon component of the shower. This question of the composition of the particles in the multiple-production event will be discussed in the next section.

It is appropriate to note that if one neglects the altitude dependence of the number of particles in the shower, one can reach an erroneous conclusion regarding the acceptability of a model for description of experimental data. For example, it can be seen in Fig. 25 that the calculated values of the number of muons and the number of electrons for a primary energy  $\sim 7.9 \cdot 10^4$  TeV and a model with a dependence  $n = 2.04 \ln E - 3.04$  correspond to experiment at a fixed depth  $\sim 800$  g/cm<sup>2</sup>.

During recent years time-analysis methods for the various components of extensive air showers have been intensively developed in an attempt to discover the pattern of development of the shower with depth in the atmosphere. It has been shown theoretically<sup>83</sup> that the cascade curve characterizing the longitudinal development of a shower of electrons in extensive showers in the atmosphere can be uniquely related to the rise and fall with time of the Cherenkov flash of the shower at distances of several hundred meters from the axis. In Fig. 26 we have shown the dependence of the duration of the Cherenkov pulse at half-height on the distance according to data obtained at the Yakutsk installation for extensive air showers with a primary energy  $\sim 10^5$  TeV and the results of a calculation of the corresponding dependences for various models of the multiple-production event.<sup>84</sup> As before, the experiment agrees with the model for a high multiplicity of hadrons in the event.

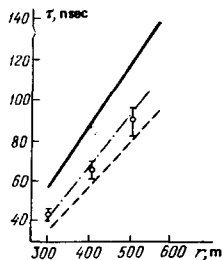


FIG. 26. Duration of Cherenkov flash as a function of distance from the axis of a large shower.<sup>84</sup> The expected dependences for various models of multiple production are shown by the straight lines: solid line—scaling, dot-dash—model with  $n \sim E^{0.25}$ , dashed line—model with  $n \sim E^{0.5}$ .

Similar conclusions can be reached on the basis of the distribution of high-energy muons in the plane transverse to the shower axis (Fig. 27). The increase of the transverse momenta of the pions (or kaons) produced in inelastic collisions of hadrons with nuclei also could increase the average distances between the observed muons and the shower axis. However, the strong increase of the transverse momenta in the total flux of secondary particles necessary for explanation of the experimental data<sup>85</sup> in multiple-production events would be inconsistent with the extremely weak rise of the transverse momenta in the main flux of  $\gamma$  rays in the Pamir experiment.

The relative number of hadrons with energy  $E_h \geq 1$  TeV in extensive showers with a primary energy  $E_0 \approx 10^3$  TeV depends only weakly on the multiplicity of secondary hadrons in the event,<sup>84</sup> but it is sensitive to the value of the effective cross section for inelastic collisions of nucleons and pions with nuclei of air atoms.<sup>22</sup> The comparison of experiment with theory confirms the possibility of extrapolating the rise of the effective cross section with incident-hadron energy to the energy region  $\sim 10^3$  TeV. The number of low-energy hadrons in an extensive air shower is determined to a significant degree by the number of baryons in the multiple-production events, since low-energy pions have time to decay in the atmosphere.<sup>86</sup>

The principal conclusion of many years of research on the multiple-production process in inelastic collisions of hadrons in extensive air showers is the strong dependence of the multiplicity on the energy of the colliding hadrons. An indication of this was obtained many years ago.<sup>74,87</sup> At the present time, aside from a dependence on the physical interpretation, it has become generally accepted that there is a need to assume a strong dependence (of the type  $n_s = 2 \ln E + 0.05 E^{0.5} - 3$ , where  $E$  is in GeV) of the secondary-particle multiplicity on the energy of the interacting hadrons.

No less important, but more controversial, is the conclusion that there is an important role of other, nonpionic channels of energy transfer from the primary nucleon to the electron-proton component of the shower.

## 10. NATURE OF SECONDARY PARTICLES IN MULTIPLE-PRODUCTION EVENTS

In the energy region  $\leq 10$  TeV the composition of the hadrons produced in inelastic collisions of nucleons and pions with nuclei does not differ substantially from

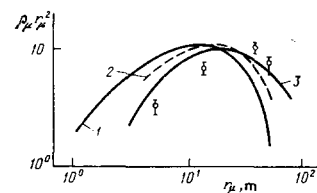


FIG. 27. Lateral distribution at sea level of muons with energy  $E_\mu > 100$  GeV in extensive air showers with primary energy  $\sim 10^3$  TeV. Curves 1 and 2—scaling, if the primary particles are protons or iron nuclei; curve 3—model with hadron multiplicity in the event  $n \sim E^{0.5}$ .

the composition of the secondary particles in multiple-production processes at accelerator energies. The greater part of the particles (~80%) are pions. The fraction of kaons can be estimated by analysis of the angular distribution of the muons in the atmosphere. For example, Varkovitskaya *et al.*<sup>88</sup> used x-ray emulsion chambers to study the angular distribution of muons with energy above 3 TeV. The corresponding effective energy of the hadrons which generate the pions and kaons, which after decay form these muons, is 40 TeV. The observed angular distribution is consistent with a fraction of kaons ~15%. This same method can be used in an attempt to estimate the fraction of short-lived hadrons (for example, charmed hadrons), which produce muons as the result of their decay. However, the results of analyses published up to the present time are contradictory. In Ref. 89 by comparison of the results of various experiments on the horizontal and vertical fluxes of muons<sup>31,35</sup> it is found that the fraction of muons of "direct production" relative to the pions at primary-hadron energies ~10 TeV should be  $R = 3\%$ . By direct-production muon we mean the production of muons through short-lived particles when it is not necessary to take into account processes which compete with the decay. In the framework of one experiment with x-ray emulsion chambers the permissible fraction of direct-production muons is limited to a value  $R = 0.8\%$ .<sup>34</sup> It should be noted that the value  $R = 3\%$  apparently cannot be provided by charmed particles, since with the probabilities known at the present time for decay of charmed particles into muons in order to obtain  $R = 3\%$  it is necessary to assume that charmed particles comprise 30–50% of the secondary particles in inelastic collisions of hadrons at energies 10–30 TeV. This is hardly likely if we do not invoke new, rapidly decaying particles with a high probability of decay by the muon channel.

The search for muons generated in dense matter by high-energy hadrons was undertaken by Bazarov *et al.*<sup>90</sup> in study of cosmic-ray extensive air showers. Spark chambers placed in the center of a comprehensive installation under an earth layer ~20 mwe were used to observe muon pairs whose tracks when extended upward converged to a point. The points of generation of the muon pairs were concentrated near the surface of the Earth or in the ionization calorimeter located on the surface above the spark chambers. Such pairs substantially exceeded in number the various background phenomena and were interpreted as muon pairs generated by high-energy hadrons near the axis of extensive air showers, not directly, but through rapidly decaying particles (for example,  $J/\psi$  particles). The effective cross section for production of such muon pairs by hadrons with energy 5–20 TeV is estimated as ~0.2 mb/nucleon. As the result of further analysis of the experimental data and corresponding nuclear-cascade calculations this estimate should be increased to ~1 mb/nucleon.<sup>91</sup> The authors of this analysis do not give this value, but give the value  $R \approx 0.2\%$ . Here they mean by  $R$  the ratio of "direct production" of a pair of muons (and not one, as before) to the number of charged pions in an event. All the  $R$  values mentioned give an effective cross section at least two orders of magnitude

larger than is known for production of  $\psi$  particles in hadron collisions at accelerator energies. This indicates a rapid rise of the effective cross section for production of particles with hidden charm and other new particles in the super-accelerator energy region.

More direct searches for new short-lived particles have been undertaken by means of a specially developed emulsion chamber. The upper part of the chamber consisted of two-sided emulsion plates, target plates of materials with low atomic number, and air gaps; the lower part of the chamber was made of emulsion plates, x-ray films, and thin lead plates. High accuracy of assembly made it possible to measure relative angles between tracks of charged secondary particles generated in the chamber with an accuracy ~ $10^{-5}$  rad. The principle of the combined use of nuclear emulsions and the target material was proposed much earlier.<sup>92</sup> As long ago as 1971 Niu *et al.*<sup>93</sup> recorded the decay of a particle, named the X particle, with a mass 2–3 GeV/ $c^2$  and a lifetime ~ $10^{-13}$  sec. Subsequently this event was interpreted as the observation of a charmed particle.<sup>94</sup> In Table VI we have given a summary of events recorded in experiments of various authors and identified as X particles in a review by Niu.<sup>95</sup> The lifetime for neutral  $X^0$  particles can be estimated as  $\sim(3-5) \cdot 10^{-13}$  sec, and that for charged  $X^\pm$  particles as  $(1-2) \cdot 10^{-12}$  sec. The probability of production is of the order of one particle pair per 20–40 multiple-production events in the energy region above 10 TeV, which leads to a cross section for X-particle production 1–4 mb/nucleon.

With increase of the energy of the interacting particles, the effective cross section for production of X particles continues to rise. This follows from analysis of data of one of the x-ray emulsion chambers at Mount Chacaltaya.<sup>100</sup> Cases were selected of interactions in the upper carbon target (see Fig. 1) of hadrons from hadron jets with a total energy in electron-photon cascades  $\sum E_\gamma \approx 15$  TeV. This corresponds to an average energy of the incident hadron ~100 TeV. The further analysis reduced to a search among jets from  $\gamma$  rays and electrons in the lower x-ray emulsion block for events in which the direction of jet with allowance for the measurement errors did not extend to a point of

TABLE VI. Energy of interaction (experiment).

Energy of interaction (experiment)	Decay range, cm	Type of decay	Particle mass, GeV/ $c^2$	Lifetime, $10^{-13}$ sec
10 TeV <sup>93</sup>	1.38	$X^\pm \rightarrow \pi^0 + x^\pm$	2–3.5	0.27–0.42
	4.88	$X^\pm \rightarrow x^0 + x^\pm$		
20 TeV <sup>92</sup>	7.3	$X^0 \rightarrow \pi^0 + x^0$	~3	~15
	2.5	$X^0 \rightarrow \pi^0 + x^0$		
25 TeV <sup>96</sup>	7.63	$X^\pm \rightarrow \eta^0 + x^0 + X^\pm$	~3	~20
	1.0	$X^\pm \rightarrow x^\pm + x^0$		
20 TeV <sup>97</sup>	8.9	$X^\pm \rightarrow x^\pm + x^0$	> 2	< 56
	8.4	$X^0 \rightarrow \pi^0 + x^0$		~7
	1.1	$X^\pm \rightarrow X^\pm + x^0$		6
	0.063	$X^\pm \rightarrow x^\pm + x^0$		0.4
	1.1	$X^0 \rightarrow \pi^0 + x^0$		0.05
	6.14	$X^0 \rightarrow \pi^0 + x^0$		~1.2
20 TeV <sup>98</sup>	1.18	$X^\pm \rightarrow x^\pm + x^0 + \gamma$	> 1.5	~1.4
	1.6	$X^\pm \rightarrow x^\pm + x^0$		~5
	1.6	$X^\pm \rightarrow x^\pm + x^0$		~10
	0.79	$X^\pm \rightarrow x^\pm + x^+ + x^- + x^0$		~10
	0.27	$X^\pm \rightarrow x^\pm + x^0$		~5
	3.04	$X^\pm \rightarrow \eta^1 + x^\pm$		~1
10 TeV <sup>99</sup>	6.34	$X^\pm \rightarrow \pi^0 + x^\pm$	1.66–2.23	5.1
			1.74–2.36	34

production in the carbon target under the upper x-ray emulsion block, but could be associated with this point by assumption of decay of an X particle in the 1.5 m air gap between the upper and lower chamber blocks. The four cases of such jets found in 12 analyzed interaction events are not comparable in probability with all the background phenomena which have been discussed. The estimates of the transverse momentum in the decay ( $\geq 1$  GeV/c) and of the lifetime ( $10^{-13}$ – $10^{-12}$  sec) are close to the corresponding characteristics of X particles in the experiments of Ref. 95. The probability of production of X particles in this experiment for incident-hadron energies 50–100 TeV can be estimated as  $4 \cdot 0.5/12 \approx 16\%$ , where the coefficient 0.5 takes into account that in selection of events for analysis one of the additional selection criteria (high multiplicity and increased average transverse momentum as in SH-quant) excludes  $\sim 50\%$  of all cases of inelastic collisions in this energy interval. It should be noted that in this case, as in Ref. 95, it is assumed that X particles can be both charmed and new heavy hadrons. The effective cross section  $\sim 10$  mb/nucleon obtained in this way for new particles is, of course, only a lower limit, since for its evaluation one compares individual cases of observation, successful in their geometry, with the total number of interactions in the target without taking into account the efficiency of the search.

A number of studies<sup>101–103</sup> using the method of detecting delayed particles in extensive air showers have observed single events of relatively stable hadrons with a mass exceeding  $5$  GeV/ $c^2$ . The lifetime of these hadrons is estimated as  $\tau_0 > 10^{-7}$  sec. Taking into account the very low upper limit for production of hadrons with mass  $5$ – $10$  GeV/ $c^2$  in the accelerator energy region, we must assume that the observed relatively stable hadrons with mass  $> 5$  GeV/ $c^2$  and energy of tens of GeV are produced in inelastic collisions in the superaccelerator energy region. As the calculations of Goodman *et al.*<sup>102</sup> show, the cross section for production of these particles in interactions at  $\sim 100$  TeV should be about  $50$   $\mu$ b.

Analyzing nuclear cascade showers in a calorimeter, Anoshin *et al.*<sup>104</sup> have suggested that heavy unstable particles with mass  $10$ – $20$  GeV/ $c^2$  and lifetime  $(5$ – $8) \cdot 10^{-11}$  sec are produced in inelastic collisions of hadrons at energies  $\geq 300$  GeV.

Of course, the absence of accelerator data on particles allegedly observed in cosmic rays at energies of hadron collisions which have been very thoroughly investigated in accelerators does not increase our confidence in this hypothesis. Therefore it is appropriate to present the main arguments for the above hypothesis, drawing on a detailed report of the essence of the experiment.<sup>105</sup> For several reasons, from all hadron cascades in the calorimeter, cases were selected of cascade curves with two maxima, in which the energy corresponding to the second maximum in depth had to exceed half of the total energy of the cascade. Experimentally this selection leaves less than  $20\%$  of the cascades of a given energy. Apart from a dependence on the selection which was carried out, the distribution of depths of the beginning of the cascades in the cali-

meter should correspond to an exponential with the interaction range of nucleons or pions in the calorimeter. This is observed for showers with a total energy less than  $200$  GeV. The distributions of the depths of generation of cascades for cases with energy above  $400$  GeV is shown in Fig. 28. To explain the excess of cascades beginning at a depth  $\geq 2$  hadron interaction ranges, the authors of Ref. 104 proposed a new process of the production of two T particles with masses  $\geq 10$  GeV/ $c^2$  in an unobserved interaction of a hadron with an iron nucleus in the upper part of the calorimeter. The decays of the particles give two maxima in the cascade, and the unobservability of the interaction in which they were generated is explained by the fact that either the two particles carry away all the energy of the interaction near the production threshold or part of the interaction energy is carried away by several particles without production of  $\pi^0$  mesons. An alternative explanation of such cascades beginning in the depth of the calorimeter could be few-particle inelastic collisions  $p+A \rightarrow n\pi^+ + A$  or  $p+A \rightarrow p\pi^+\pi^-$ , which also are recorded among the secondary interactions in the depth of the calorimeter. Dem'yanov *et al.*<sup>105</sup> point out a number of features which make it preferable to assume the production of T particles. These are: the slow absorption of the showers, which is related to the cascade decay of the T particles, and the disappearance of events with two maxima beginning in the interior of the calorimeter in the transition to higher cascade energies.

The effective cross section for production of T particles is estimated from the distribution in Fig. 28 with allowance for the selection of hadron cascades with two maxima as  $\sim 2$  mb/nucleon at generating-hadron energies  $\sim 400$  GeV. It rises with energy up to  $6$ – $10$  mb/nucleon at  $1$  GeV.

## 11. ROLE OF NEW PARTICLES IN HADRON CASCADES

The numerous experimental data presented in the preceding section differ greatly in their reliability. However, they direct our attention to an important characteristic feature of inelastic collisions in the superaccelerator energy region: the new particles become completely nonexotic in their probability of appearance, and the effective cross section for their production continues to rise with increase of the energy of the interacting hadrons.

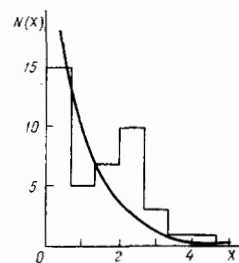


FIG. 28. Distribution of depths of generation of hadron cascades in the calorimeter for cascade energies above  $400$  GeV. The curve shows the expected distribution.

How is this reflected in the properties of the hadron cascade in the atmosphere and in dense matter? Should we be happy with the agreement between the experimentally observed characteristics and calculations in which the changed composition of the particles in multiple-production events is not taken into account? To answer these questions is still difficult, since at the present time our ideas regarding the nature and properties of the new particles have a particularly hypothetical nature.

In the preceding sections we have given examples of the fact that, without taking into account production in inelastic hadron collisions of particles other than pions, nucleons, and kaons it is impossible to explain a number of phenomenological characteristics of the passage of cosmic rays through the atmosphere or the lead of the ionization calorimeter.

To explain the angular distribution of muons with energy  $\geq 1$  TeV, direct production of muons was assumed. Here particles which decay with a charmed-particle lifetime are completely equivalent to direct production of muons.

Exotic phenomena such as centaurs and geminions may be related to the production of new particles of large mass (tens of  $\text{GeV}/c^2$ ) and lifetime less than  $10^{-11}$  sec.

The relations between the different components of extensive air showers require for their explanation some preference in transfer of energy to the electron-photon component in comparison with the distribution known from accelerator data of the energy between nucleons, kaons, and charged and neutral pions (gammanization). This was investigated quantitatively by D'yakonov *et al.*<sup>106</sup> by variation of the ratio of the total energies of charged and neutral pions produced in heavy fireballs. The experiment which relates the primary energy at  $10^5$ – $10^6$  TeV, the number of electrons in a shower at sea level, and the number of muons is in agreement with the ratio  $\sum E_{e\gamma} / \sum E_{\mu} = 0.39$  instead of 0.33.

The anomalies in the absorption of hadron cascades in the calorimeter (see Fig. 12) are unexplainable without the assumption that in inelastic collisions at incident-hadron energies  $\geq 100$  TeV new particles are formed and that the slow absorption of these particles as the result of inelastic interactions or decay protracts the absorption of ordinary nucleon-pion cascades. However, if we assume for the new particles the usual exponential absorption, as for inelastic interactions (or decay), then it is necessary to assume for the quantitatively observed absorption at hadron energies  $\geq 100$  TeV that more than half of the energy of the incident hadron goes into the new particles. Decreasing this energy, i.e., substantially distorting the exponential nature of the absorption of the new particles, is possible only by assuming cascade decay of the particles which are leading in energy (the fragmentation part of the secondary-particle energy spectrum). The decay of some kind of particles produced in collision of the primary protons and nuclei with the nuclei of air atoms at energies  $\geq 10^3$  TeV is apparently manifested also in the rapid shift of the height of the maximum of develop-

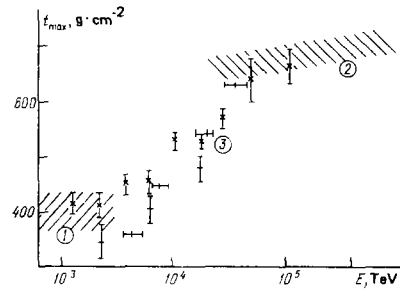


FIG. 29. Depth of maximum of development of electron-photon component of extensive air showers in the atmosphere as a function of the energy of the primary particle. The experimental data (1) were obtained in direct measurements,<sup>74,80</sup> the data (2) are from Ref. 75, and the data (3), which have been published in two different articles,<sup>107,108</sup> were obtained by analysis of the duration of the Cherenkov flash on passage of a shower through the atmosphere.

ment of the electron-photon component of the shower (Fig. 29). In Ref. 107 this rapid shift of the maximum was related to a change in the composition of the primary cosmic radiation from a predominant flux of iron nuclei at  $10^3$  TeV to almost solely protons at  $10^5$  TeV. However, studies of fluctuations in extensive air showers exclude any dominance of iron nuclei at  $10^3$  TeV.

However, if we assume, as for explanation of anomalies in the absorption of hadron cascades in lead, that in interactions of primary protons and nuclei in their initial path in the atmosphere a substantial part of the energy is somehow transferred to unstable particles, then the shift of the maximum of the development of extensive air showers in height in the region of energies  $3 \cdot 10^3$ – $3 \cdot 10^4$  TeV permits estimation of the lifetime of the particles or some characteristic cascade decay length. We shall assume that for incident-hadron energies above 100 TeV in a multiple-production event in addition to pions, nucleons, and kaons, and unstable particle with a lifetime  $\tau_0$  and energy  $\alpha E_0/A$  is formed. Here  $A$  is the average atomic number of the primary particles with energy  $E_0$ , the nucleons of which transfer a fraction  $\alpha$  of their energy to a particle with mass  $M$ . For primary energies  $E_0 < 10^4$  TeV these particles decay in a path of less than 300 m, and thereby increase the effective multiplicity of secondary particles after the first multiple-production events and accelerate the development of the electron-photon component of the shower. With increase of the energy  $E_0$  the decay range increases up to the range for inelastic collisions of nucleons in the atmosphere and even higher. In this way the presence of the new particles at energies  $\geq 6 \cdot 10^4$  TeV already does not accelerate the development of the shower in the atmosphere and may even slow it down. The corresponding conditions for  $\alpha = 0.5$  and  $A = 10$  ( $3 \cdot 10^5$  GeV/ $M$ )  $\tau_0 c < 3 \cdot 10^3$  cm and ( $3 \cdot 10^6$  GeV/ $M$ )  $\tau_0 c \geq 3 \cdot 10^5$  cm lead to  $\tau_0 \approx 3 \cdot 10^{-12} M$  sec, where  $M$  is the mass in  $\text{GeV}/c^2$ .

The assumption of a value  $\alpha = 0.5$  in the simultaneous production of pions and other hadrons means that the inelasticity coefficient of nucleons in inelastic collisions at energies above 100 TeV increases and ap-

proaches unity. The existing experimental data are consistent with this assumption. In many cases the experimental data on extensive air showers with primary energy above  $10^3$  TeV are reconciled with calculations most simply on the assumption that the inelasticity coefficient in this energy region is 1. However, as yet there are no direct experimental data on the inelasticity coefficient at incident-nucleon energies above 50 TeV, nor is there an analysis of experimental data which uniquely demonstrates the need of such an assumption. It is not excluded that this very important question will be clarified only in accelerator experiments.

## 12. CONCLUSION

The set of data presented above which were obtained from experiments in cosmic rays permits formulation of a number of basic properties of inelastic collisions and multiple production of hadrons in the energy region  $1-10^6$  TeV.

1. The effective cross section for inelastic collisions of nucleons with nuclei of air atoms rises with increase of the incident-nucleon energy and in the energy region  $10^3 \leq E \leq 10^9$  GeV can be represented as

$$\sigma_{\text{prod}}^{\text{air}} = 270 \left[ 1 + 0.016 \left( \ln \frac{E}{80} \right)^{1.5} \right] \text{ (mb)}.$$

2. The multiplicity of secondary hadrons produced in inelastic hadron collision at energies  $E \geq 10^3$  GeV increases as

$$n_s = 2 \ln E + 0.05E^{0.5} - 3.$$

3. The energy spectrum of secondary hadrons in multiple-production events is consistent with a distribution of the Bose-Planck type if it is supplemented by diffraction processes which do not fall off with increase of the energy.

4. In the energy region below 50 TeV the distribution of the inelasticity coefficient in interactions of nucleons with nuclei does not change with change of the incident-nucleon energy and depends only weakly on the atomic number of the target nucleus.

5. The distributions of transverse momenta of the greater part of the secondary pions in multiple-production events are practically unchanged in the incident-particle energy region below 100 TeV and rise only weakly at higher energies.

6. In the energy region below 50 TeV the composition of the secondary particles changes only slightly. For incident-nucleon energies above 100 TeV, new particles are generated with an effective cross section  $(0.3-0.5)\sigma_{\text{prod}}$  which carry away on the average more than 30% of the energy of the initial nucleon, apparently as the result of leading nucleons and pions.

7. The new particles have an inelasticity coefficient and (or) an effective cross section several times smaller than nucleons and pions and may decay with formation of a cascade of decays with a lifetime  $\tau_0 \approx 3 \cdot 10^{-12}$  sec by hadron and lepton channels.

8. In the incident-hadron energy region above 100 TeV the probability of production of particles and jets

with large transverse momenta ( $>1$  GeV/c) increases substantially. It is possible that this should be related to the production and decay of new particles of large mass.

Now we can consider the general picture of inelastic collisions of hadrons in the energy region  $1-10^6$  TeV. Why can we or even must we speak of a difference of processes below and above  $10-100$  TeV?

The energy region up to 50 TeV can be considered completely as a region of approximate scale invariance, quasiscaling, which is characterized by preservation of the peripheral nature of inelastic collisions, constancy of the inelasticity coefficient of the colliding nucleons, secondary-particle transverse momenta which essentially do not depend on the initial energy, and a constant composition of the greater part of the secondary particles.

Scaling violations appear in the rise of the effective cross section for inelastic collisions, and in the strong dependence of the multiplicity of the hadrons of the pionization part of the inclusive spectrum on the incident-hadron energy. The increase of the number of charmed and other new hadrons at incident-hadron energies of  $10-30$  TeV is apparently a precursor of changes in the multiple-production process at energies above 50 TeV.

In the energy region  $\geq 100$  TeV inelastic collisions of hadrons are characterized by a more rapid rise of the secondary-hadron multiplicity with increase of the interaction energy, an absence of scale invariance even in the fragmentation part of the secondary-particle spectrum, a rise of the effective cross section for production of hadrons and hadron jets with large transverse momenta, and a substantial, energetically significant change in the composition of the secondary hadrons.

We can suppose that with increase of the energy of the colliding hadrons there is an increase in the probability of formation of clusters (fireballs) of large mass. However, under this assumption the significant increase of the effective cross section for particles other than pions, kaons, and nucleons, the large transverse momenta, and especially the violation of scaling in the fragmentation part of the secondary-particle spectrum—all these factors require additional changes in the multiple-production process.

The more fundamental assumption that at energies above 100 TeV particles with large masses, tens of GeV/c<sup>2</sup>, are produced or that quarks are liberated, immediately includes, as a manifestation of this process, cascades of decays of the new particles, large transverse momenta, changes in the fragmentation of the colliding hadrons, and an effective increase in multiplicity, if not directly in the event, then in subsequent decays of the fragmentation particles.

Of course, the existing experimental data are insufficient for construction and verification of a physical model of the new processes which accompany inelastic collisions of hadrons in the energy region above 100

TeV. The new generation of accelerators with colliding beams is aimed at this interesting energy region, and we can expect a transition to the next stage in understanding of the structure and properties of hadrons. In addition, detailed characteristics of inelastic proton-proton and proton-antiproton collisions in the energy region  $10^2$ – $10^3$  TeV will be a reliable base for further advance along the energy scale in studies of hadron-nucleus interactions in cosmic rays.

I am grateful to N. A. Dobrotin, I. M. Dremin, A. D. Erlykin, V. A. Tsarev, V. I. Yakovlev, and especially to E. L. Feinberg for helpful discussions and numerous remarks on the first version of this article.

<sup>1</sup>C. M. G. Lattes *et al.*, ICR Report-81-80-3. Inst. Cosmic Ray Research, University of Tokyo, 1980.  
<sup>2</sup>Pamir Collaboration, Zeszyty Naukowe Uniwersytetu Lodzkiego, Ser. II, 1977, Vol. 60 p. 7.  
<sup>3</sup>T. P. Amineva *et al.*, Trudy FIAN SSSR (Proceedings of the Lebedev Institute) 46, 157 (1970).  
<sup>4</sup>N. L. Grigorov, I. D. Rapoport, and V. Ya. Shestoporov, Chastitsy vysokikh énergii v kosmicheskikh luchakh (High Energy Particles in Cosmic Rays), Moscow, Nauka, 1973.  
<sup>5</sup>M. Simon *et al.*, Sixteenth ICRC<sup>2)</sup> Papers, 1, 352 (1979).  
<sup>6</sup>M. J. Ryan *et al.*, Phys. Rev. Lett. 28, 985 (1972).  
<sup>7</sup>D. D. Krasilnikov *et al.*, Fifteenth ICRC Papers 8, 159 (1977).  
<sup>8</sup>O. S. Diminstein *et al.*, Fourteenth ICRC Papers 12, 4318 (1975).  
<sup>9</sup>A. R. Clarke *et al.*, Fourteenth ICRC Papers 8, 2699 (1975).  
<sup>10</sup>R. G. Brownlee *et al.*, Fourteenth ICRC Papers 8, 2704 (1975).  
<sup>11</sup>S. N. Vernov *et al.*, Can. J. Phys. 46, S197 (1968).  
<sup>12</sup>S. I. Nikol'skii, Izv. AN SSSR, Ser. fiz. 39, 1160 (1975) [Bull. USSR Acad. Sci., Phys. Ser.].  
<sup>13</sup>A. M. Hillas, Sixteenth ICRC Papers 8, 7 (1979).  
<sup>14</sup>S. I. Nikolsky *et al.*, Sixteenth ICRC Papers 8, 335 (1979).  
<sup>15</sup>S. I. Nikol'skii, in: Kosmicheskie luchy i problemy kosmofiziki (Cosmic Rays and Problems of Cosmic Physics), Novosibirsk, Siberian Division, USSR Academy of Sciences, 1964, p. 87.  
<sup>16</sup>S. I. Nikolsky *et al.*, Seventeenth ICRC Papers 2, 129 (1981).  
<sup>17</sup>R. J. Glauber, in: High Energy Physics and Nuclear Structure/Ed. S. Devons, N.Y., Plenum Press, 1970.  
<sup>18</sup>R. A. Nam *et al.*, Yad. Fiz. 26, 1038 (1977) [Sov. J. Nucl. Phys. 26, 550 (1977)].  
<sup>19</sup>T. K. Gaisser *et al.*, Fourteenth ICRC Papers 7, 2161 (1975).  
<sup>20</sup>N. N. Kalmykov *et al.*, Sixteenth ICRC Papers 9, 73 (1979).  
<sup>21</sup>G. B. Kristiansen *et al.*, Izv. AN SSSR, Ser. fiz. 40, 987 (1976) [Bull. USSR Acad. Sci., Phys. Ser.].  
<sup>22</sup>I. P. Ivanenko *et al.*, Yad. Fiz. 29, 694 (1979) [Sov. J. Nucl. Phys. 29, 358 (1979)].  
<sup>23</sup>Y. Mitsumoto *et al.*, Sixteenth ICRC Papers 9, 116 (1979).  
<sup>24</sup>V. P. Pavlyuchenko *et al.*, Trudy FIAN SSSR (Proceedings of the Lebedev Institute) 109, 30 (1979).  
<sup>25</sup>A. I. L'vov *et al.*, Izv. AN SSSR, Ser. fiz. 44, 491 (1980) [Bull. USSR Acad. Sci., Phys. Ser.].  
<sup>26</sup>L. V. Volkova *et al.*, Yad. Fiz. 29, 1252 (1979) [Sov. J. Nucl. Phys. 29, 645 (1979)].  
<sup>27</sup>K. Kasahara, Fifteenth ICRC Papers 7, 395 (1977).  
<sup>28</sup>A. M. Dunaevskii *et al.*, Fifteenth ICRC Papers 7, 337 (1977).  
<sup>29</sup>A. D. Erlykin *et al.*, Preprint of P. N. Lebedev Physical Institute, No. 95, Moscow, 1980.  
<sup>30</sup>E. A. Kanevskaya *et al.*, Fifteenth ICRC Papers 7, 453 (1977).  
<sup>31</sup>M. G. Thompson *et al.*, Sixteenth ICRC Papers 10, 59 (1979).

<sup>2)</sup> ICRC—International Cosmic Ray Conference.

<sup>32</sup>O. C. Allkofer *et al.*, Twelfth ICRC Papers 4, 1319 (1971).  
<sup>33</sup>B. Baschiera *et al.*, Sixteenth ICRC Papers 13, 330 (1979).  
<sup>34</sup>U. A. Ivanova *et al.*, Sixteenth ICRC Papers 10, 35 (1979).  
<sup>35</sup>K. Honda *et al.*, Sixteenth ICRC Papers 10, 59 (1979).  
<sup>36</sup>O. C. Allkofer *et al.*, Sixteenth ICRC Papers 10, 50 (1979).  
<sup>37</sup>I. P. Ivanenko *et al.*, Sixteenth ICRC Papers 7, 101 (1979).  
<sup>38</sup>C. M. G. Lattes *et al.*, Thirteenth ICRC Papers 3, 2219 (1973).  
<sup>39</sup>Pamir ECC Group, Fourteenth ICRC Papers 7, 2365 (1975).  
<sup>40</sup>E. A. Kanevskaya *et al.*, Fifteenth ICRC Papers 7, 452 (1977).  
<sup>41</sup>M. Akashi *et al.*, Sixteenth ICRC Papers 7, 68 (1979).  
<sup>42</sup>J. Wdowczyk and A. W. Wolfendale, Nuovo Cimento Ser. A54, 433 (1979).  
<sup>43</sup>S. I. Nikol'skii, Zh. Eksp. Teor. Fiz. 51, 804 (1966) [Sov. Phys. JETP 24, 535 (1967)].  
<sup>44</sup>F. Ashton *et al.*, Fifteenth ICRC Papers 8, 6 (1977).  
<sup>45</sup>V. A. Romakhin and N. M. Nesterova, Trudy FIAN SSSR (Proceedings of the Lebedev Institute) 109, 77 (1979).  
<sup>46</sup>V. S. Aseikin *et al.*, Izv. AN SSSR, Ser. fiz. 38, 998 (1974) [Bull. USSR Acad. Sci., Phys. Ser.].  
<sup>47</sup>E. V. Bazarov *et al.*, Kr. soobshch. FIAN SSSR (Brief Communications, Physics Institute, USSR Academy of Sciences), No. 10, 15 (1980).  
<sup>48</sup>E. L. Feinberg *et al.*, Preprint of P. N. Lebedev Physical Institute, No. 69, Moscow, 1975.  
<sup>49</sup>W. E. Hazen *et al.*, Phys. Rev. 93, 578 (1954).  
<sup>50</sup>N. A. Dobrotin *et al.*, Nuovo Cimento 8, 612 (1958).  
<sup>51</sup>A. M. Bray *et al.*, Acta Phys. Hung. 29, Suppl. 3, 501 (1970).  
<sup>52</sup>S. K. Machavariani *et al.*, Seventeenth ICRC Papers 6, 193 (1981).  
<sup>53</sup>H. Sugimoto *et al.*, AIP Conf. Proc. No. 149, 126 (1979).  
<sup>54</sup>G. Charlton *et al.*, Phys. Rev. Lett. 29, 1759 (1972).  
<sup>55</sup>S. G. Bayburina *et al.*, Fifteenth ICRC Papers 7, 229 (1977).  
<sup>56</sup>M. Akashi *et al.*, Fifteenth ICRC Papers 7, 184 (1977).  
<sup>57</sup>J. N. Capdevielle *et al.*, Sixteenth ICRC Papers 6, 324 (1979).  
<sup>58</sup>Brazil-Japan Emulsion Chamber Collaboration, Sixteenth ICRC Papers 350, 145 (1979).  
<sup>59</sup>L. T. Baradzei *et al.*, Sixteenth ICRC Papers 7, 279 (1979).  
<sup>60</sup>A. E. Chudakov *et al.*, Sixteenth ICRC Papers 8, 222 (1979).  
<sup>61</sup>S. Hasegawa, Prog. Theor. Phys. 26, 150 (1961).  
<sup>62</sup>Japanese and Brazilian Emulsion Chamber Group, Canad. J. Phys. 46, 660 (1968).  
<sup>63</sup>M. Akashi *et al.*, Twelfth ICRC Papers 7, 2775 (1971).  
<sup>64</sup>K. V. Cherdyntseva *et al.*, Yad. Fiz. 9, 152 (1969) [Sov. J. Nucl. Phys. 9, 92 (1969)].  
<sup>65</sup>Brazil-Japan Emulsion-Chamber Collaboration, Fifteenth ICRC Papers 7, 208 (1977).  
<sup>66</sup>Brazil-Japan Emulsion-Chamber Collaboration, in: Bartol Conference Proceedings, N.Y., American Institute of Physics, 1979, p. 145.  
<sup>67</sup>C. Bromberg *et al.*, Phys. Rev. Lett. 38, 1447 (1977).  
<sup>68</sup>V. K. Budilov *et al.*, Fourteenth ICRC Papers 7, 2370 (1975).  
<sup>69</sup>S. G. Baiburina *et al.*, Izv. AN SSSR, Ser. fiz. 44, 450 (1980) [Bull. USSR Acad. Sci., Phys. Ser.].  
<sup>70</sup>L. T. Baradzei *et al.*, Izv. AN SSSR, Ser. fiz. 42, 1361 (1975) [Bull. USSR Acad. Sci., Phys. Ser.].  
<sup>71</sup>J. Wdowczyk *et al.*, Izv. AN SSSR, Ser. fiz. 42, 1356 (1978) [Bull. USSR Acad. Sci., Phys. Ser.].  
<sup>72</sup>S. G. Baiburina, Izv. AN SSSR, Ser. fiz. 42, 1346 (1978) [Bull. USSR Acad. Sci., Phys. Ser.].  
<sup>73</sup>J. Wdowczyk *et al.*, Izv. AN SSSR, Ser. fiz. 44, 461 (1980) [Bull. USSR Acad. Sci., Phys. Ser.].  
<sup>74</sup>R. A. Antonov *et al.*, Zh. Eksp. Teor. Fiz. 45, 1865 (1963) [Sov. Phys. JETP 18, 1279 (1964)].  
<sup>75</sup>N. N. Kalmykov *et al.*, Sixteenth ICRC Papers 9, 73 (1979).  
<sup>76</sup>Pamir Collaboration Workshop, Lodz, University of Lodz, 1980, p. 15.  
<sup>77</sup>A. K. Managadze *et al.*, Acta Universitatis Lodzianensis, Ser. II, No. 32, 197 (1980).  
<sup>78</sup>Pamir Collaboration Workshop, Lodz: University of Lodz,

- 1980, p. 94.
- <sup>78</sup>S. G. Baiburina *et al.*, *Izv. AN SSSR, Ser. fiz.* **44**, 547 (1980) [*Bull. USSR Acad. Sci., Phys. Ser.*].
- <sup>80</sup>R. A. Antonov *et al.*, *Izv. AN SSSR, Ser. fiz.* **44**, 547 (1980) [*Bull. USSR Acad. Sci., Phys. Ser.*].
- <sup>81</sup>C. Aguirre *et al.*, *Sixteenth ICRC Papers* **8**, 1078 (1979).
- <sup>82</sup>M. N. Dyakonov *et al.*, *Sixteenth ICRC Papers* **8**, 174 (1979).
- <sup>83</sup>Yu. A. Fomin *et al.*, *Yad. Fiz.* **14**, 642 (1971) [*Sov. J. Nucl. Phys.* **14**, 360 (1971)].
- <sup>84</sup>S. N. Vernov *et al.*, *Fifteenth ICRC Papers* **8**, 320 (1977).
- <sup>85</sup>B. A. Khrenov *et al.*, *Sixteenth ICRC Papers* **8**, 351 (1979).
- <sup>86</sup>T. V. Danilova *et al.*, *J. Phys. Soc., Japan, Suppl., A III*, **17**, 205 (1963).
- <sup>87</sup>I. L. Rozental', *Dokl. Akad. Nauk SSSR* **80**, 731 (1951).
- <sup>88</sup>A. Ya. Varkovitskaya *et al.*, *Izv. AN SSSR, Ser. fiz.* **44**, 602 (1980) [*Bull. USSR Acad. Sci., Phys. Ser.*].
- <sup>89</sup>Yu. A. Nechin *et al.*, *Izv. AN SSSR, Ser. fiz.* **44**, 640 (1980) [*Bull. USSR Acad. Sci., Phys. Ser.*].
- <sup>90</sup>E. V. Bazarov *et al.*, *Trudy FIAN (Proceedings of the Lebedev Institute)* **109**, 109 (1979).
- <sup>91</sup>E. V. Bazarov *et al.*, *Izv. AN SSSR, Ser. fiz.* **44**, 561 (1980) [*Bull. USSR Acad. Sci., Phys. Ser.*].
- <sup>92</sup>M. F. Kaplon *et al.*, *Phys. Rev.* **85**, 295 (1952).
- <sup>93</sup>K. Niu *et al.*, *Twelfth ICRC Papers* **7**, 2792 (1971).
- <sup>94</sup>T. Hayashi *et al.*, *Prog. Theor. Phys.* **47**, 1998 (1972).
- <sup>95</sup>K. Niu, *AIP Conf. Proc. No. 49* 181 (1979).
- <sup>96</sup>K. Nishikawa, *J. Phys. Soc., Japan* **14**, 880 (1959).
- <sup>97</sup>S. Kuramata *et al.*, *Thirteenth ICRC Papers* **3**, 2239 (1973).
- <sup>98</sup>H. Fuchi *et al.*, in: *Nineteenth Intern. Conf. High Energy Physics, Tokyo, 1977*, p. 491.
- <sup>99</sup>H. Sugimoto *et al.*, *Prog. Theor. Phys.* **53**, 1541 (1975).
- <sup>100</sup>K. Sawayanagi, *Phys. Rev. Ser. D* **20**, 1037 (1979).
- <sup>101</sup>L. W. Jones *et al.*, *Phys. Rev. Ser.* **164**, 1584 (1967).
- <sup>102</sup>J. A. Goodman *et al.*, *Phys. Rev. Ser. D* **20**, 2572 (1979).
- <sup>103</sup>P. N. Bhat *et al.*, *Sixteenth ICRC Papers* **6**, 57 (1979).
- <sup>104</sup>A. I. Anoshin *et al.*, *Pis'ma Zh. Eksp. Teor. Fiz.* **15**, 10 (1972) [*JETP Letters* **15**, 6 (1972)].
- <sup>105</sup>A. I. Dem'yanov, V. S. Murzin, and A. I. Sarycheva, *Yaderno kaskadnyi protsess v plotnom veshchestve (The Nuclear Cascade Process in Dense Matter)*, Moscow, Nauka, 1977, Chapter 7.
- <sup>106</sup>M. N. D'yakonov *et al.*, *Izv. AN SSSR, Ser. fiz.* **38**, 993 (1974) [*Bull. USSR Acad. Sci., Phys. Ser.*].
- <sup>107</sup>G. J. Thornton and R. W. Clay, *J. Phys. G5*, L137 (1979).
- <sup>108</sup>G. J. Thornton *et al.*, *Sixteenth ICRC Papers* **9**, 103 (1979).

Translated by Clark S. Robinson